Visualizing Gene Expression in *Geobacter sulfurreducens* Biofilms on Graphite Electrodes

A THESIS
SUBMITTED TO THE FACULTY OF THE GRADUATE SCHOOL
OF THE UNIVERSITY OF MINNESOTA
BY

Clint Michael Remarcik

IN PARTIAL FULFILLMENT OF THE REQUIREMENTS
FOR THE DEGREE OF
MASTER OF SCIENCE

Dr. Daniel R. Bond PhD

December 2010

Acknowledgements

Scientific knowledge cannot evolve without drawing on a foundation of knowledge. Therefore, I must thank those who have laid the groundwork for my studies. Thank you to those who have stimulated me to think critically about my studies and been there to aid in troubleshooting. Special thanks goes to the Dr. Derek Lovley lab for supplying the pRG5Mc vector. Special thanks also goes to the Imaging Center at the University of Minnesota for allowing me to commandeer the confocal microscope. Thank you to my committee members Dr. Jeffrey Gralnick and Dr. Christine Salomon for giving me constructive feedback on my project as it progressed. To my mentor Dr. Daniel Bond, your enthusiasm for science is infectious and I thank you for keeping me motivated and pushing me to be a better scientist. And lastly, thank you to my friends and family. Your encouragement has gotten me to where I am today.

Dedication

I dedicate this thesis to all those who have aided in my development as a scientist.

Abstract

The *Geobacteraceae* are a family of deltaproteobacterial anaerobes known to play important roles in environmental Fe(III)-reduction, subsurface petroleum bioremiediation, bioprecipitation of heavy metals, and reduction of anodes in microbial fuel cells. Electron transfer by *Geobacteraceae* requires formation of a multicellular biofilm, as cells must attach to surfaces or insoluble particles to bring redox proteins in contact with their electron acceptor, and growth of daughter cells requires cell-cell contact to facilitate longer-range electron transfer. The primary aim of this thesis was to develop new tools for three-dimensional visualization of gene expression within these biofilms. To detect differential expression in a developing biofilm, the genetically tractable representative *Geobacter sulfurreducens* was utilized as a model. Promoters from two *c*-type cytochromes proven to be important in electron transfer were inserted upstream of the fluorescent protein mCherry, or a derivative of mCherry containing an additional peptide sequence (LVA) to accelerate protein degradation and act as a signal of more recent expression. Control plasmids containing no mCherry, or with the fluorescent protein under control of a constitutive *taclac* promoter were also transformed into *G. sulfurreducens*. The plasmid backbone used for expression was found to affect growth of cells as biofilms, and a new mobilizable plasmid was developed for use in these experiments. Cells had to be exposed to oxygen for four hours to achieve maximum fluorescence, indicating that future real-time studies with these proteins reliant on oxygen leakage into biofilms would not be reliable. In addition, as *G. sulfurreducens* was found to possess significant background fluorescence when grown as a biofilm in the same emission range as mCherry, future studies should investigate reporters that operate at different wavelengths. After correcting for these effects, it was demonstrated the promoter for *omcZ* was expressed fairly uniformly throughout the biofilm, with localized pockets of high expression. The promoter for *omcS*, was expressed at significantly higher levels towards the top of the biofilm when biofilms were at maximum thickness (>20 μm). These results demonstrate that promoter-reporter fusions can be used for visualization of cytochrome expression in *G. sulfurreducens* biofilms, and highlights numerous issues related to plasmid choice, protein oxidation, and background fluorescence which could create artifacts and confound results.

Table of Contents

List of Tables

List of Figures

Chapter 1

Introduction

Much interest has been given to biofilms and their development. Biofilms are aggregations of microorganisms that attach to a surface and usually have an associated extracellular matrix. Medically, biofilms are important for their role in pathogenesis [1]. More recently, they have received attention for their role in renewable energy production, as some biofilm-forming bacteria are able to couple the oxidation of organic substrates to the reduction of insoluble electron acceptors. These bacteria can be described as dissimilatory metal reducing bacteria (DMRB) [2]. *Geobacter sulfurreducens*, a DMRB, has been studied extensively for its ability to produce relatively high currents (1 mA/cm^2) when grown on graphite electrodes [3]. Understanding the key properties of *G. sulfurreducens* biofilms is instrumental in describing their ability for high current production.

Studies have shown that *c*-type cytochromes are involved in the extracellular transfer of electrons at high current densities [4]. The *G. sulfurreducens* genome encodes over a hundred *c*-type cytochromes. Transcription analysis and gene knockouts have elucidated the importance of some of these proteins in current production [5, 6]. Two cytochromes, OmcZ and OmcS, are the focus of this thesis. OmcZ, a cytochrome loosely attached to the outer surface membrane, has been shown to be required for electron transfer to electrodes [7]. It has also been shown to be a part of the extracellular matrix, possibly associated with the pili or extracellular polysaccharides [8]. Another cytochrome, OmcS, is shown to be associated with pili on the cell's outer surface [9].

While recent biochemical data has suggested where on a cell these proteins are localized, little data exists to indicate if these cytochromes are specifically expressed at different locations within a biofilm. Microtoming of an electricity producing biofilm coupled to transcription analysis was recently performed to determine if differential expression occurs in *G. sulfurreducens* biofilms. The upper portion of the biofilm (30-60 μm) was found to have lower levels of growth rate dependent genes compared to the lower portion (0-20 μm), but differential expression of *c*-type cytochromes was not observed between the two slices [10]. This conflicts with recent antibody labeling studies which observed higher levels of OmcZ protein near the base of current-producing biofilms [11]. Therefore, new methodology may be needed to visualize gene expression in *G. sulfurreducens* biofilms at higher resolution. It has been proposed that biofilms are dynamic, going through distinct changes depending on the microenvironment that challenges the biofilm [12]. The dynamics of development and gene expression have been visualized in biofilms of many bacteria by utilizing promoter-reporter fusions. In particular, the demonstration of differential gene expression in mixed aerobic-anaerobic biofilms of *Shewanella oneidensis*, another metal-reducing bacterium, provides a proof-of-concept for further work in *Geobacter* [13].

Promoter-reporter fusions can be powerful tools for assessing gene regulation. When a promoter of interest is fused to a gene encoding a fluorescent protein, expression can be quantified and/or visualized in three dimensions. For example, the strength of numerous *Escherichia coli* promoters have been quantified [14] and anaerobic metabolism in a developing biofilm visualized [13]. The promoter-reporter system allows

for the ability to visualize gene expression in real time with high resolution. A key hypothesis of this project was that through the use of promoter-reporter fusions, gene expression in a developing *Geobacter* biofilm could be visualized on a micron scale. Furthermore, through the use of unstable reporter genes, the expression of certain promoters will be able to be visualized both temporally and spatially in current-producing *G. sulfurreducens* biofilms.

Introduction to Microbial Fuel Cells (MFCs)

The use of alternative, renewable energies is necessary to curb our consumption of fossil fuels. Many technologies have been and are currently being studied and employed. Microbial fuel cells (MFC) have gained increasing popularity for their ability to use microorganisms as catalysts; coupling the degradation of organic wastes, biomass, and other carbon sources to the production of electricity [15]. MFCs are often constructed as chambered devices that separate the microbial oxidation of organic and inorganic substrates and reduction of an oxidizing species into different chambers. As electrons are liberated from substrates via metabolism in the anodic chamber they flow from the anode to the cathodic chamber. The electrons encounter a resistor or are operated under a load so that the current can be harvested for use. In order to balance charge transfer, a proton-permeable membrane (PEM) is used. This membrane is designed to exclude any substrate or cathodic electron acceptor from diffusing through. Protons produced in the anodic chamber flow to the cathodic chamber and combine with the electrons transferred to the cathode. A suitable oxidizing species is used to oxidize the cathode allowing further

reactions/current production to continue. Anodic chambers are often maintained anaerobically so that oxygen does not interfere with current production, but oxygen may serve to oxidize the cathode [16].

A variety of materials can be used for the cathode and anode. Anodes must be able to withstand the reaction conditions, be populated by microorganisms, and preferably made from highly conductive material. Some examples of anode material are gold, metal oxides, and carbon (graphite, felt, and glassy). Carbon electrodes are of interest because they are inexpensive and have a defined and often increased surface area so current density can be quantified or current production maximized. Cathode materials are chosen so that the kinetics of reducing the oxidizing species at the cathode surface is fast and complete. Because oxygen is usually used as the oxidant, platinum is typically used as the cathode. An attractive feature of platinum is that it is highly conductive and easily recovered from oxidation. A drawback is that it is expensive, so other materials are often investigated as substitutes. In this study a modified cell is constructed in which the anode and cathodes share one chamber, and a potentiostat is used to drive reduction at the cathode, eliminating the need for a PEM and oxidant [17].

In a single-chambered electrolysis cell the entire cell can be kept anaerobic and a reference electrode included to allow a potentiostat to maintain the potential at the anode. Along with the materials used, the choice of microorganism that will be catalyzing reduction of the anode is important. Many microorganisms may be able to metabolize the desired substrate, but they also need to transfer electrons to the anode as their electron acceptor. In order to accomplish extracellular electron transfer to the anode, bacteria

capable of respiring insoluble acceptors are utilized. By eliminating oxygen and other acceptors the DMRB is forced to transfer electrons extracellularly to the anode.

Dissimilatory metal-reducing bacteria (DMRB)

DMRB are important in the environmental cycling of organic compounds and metals, and reduction of environmental Fe(III) by DMRB is of particular importance. Iron is one of the most abundant elements on Earth and is utilized in a number of important biochemical reactions. In aquatic and subsurface environments, Fe(III) is in great abundance for potentially accepting electrons in organic decomposition [2]. DMRB actively reduce Fe(III) to Fe(II), and it is suggested that the majority of Fe(III) reduction in iron-rich environments (anaerobic soils, aquatic sediments, and aquifers) is performed by DMRB [18]. Not only does reduced Fe(III) affect the iron speciation in sediments and aquifers but can also affect levels of organic contaminants in the environment [19, 20]. DMRB have also been implicated in bioremediation of heavy-metal contaminated environments. The same physiology that allows for Fe(III) reduction allows for the reduction of U(VI) to U(IV) [18]. When oxidized, U(VI) is soluble and mobile in the groundwater, which poses concern for contamination, namely for drinking water. However, when reduced, it tends to form insoluble precipitates. The ability of DMRB to precipitate heavy metals and radionuclides has led to their use at contaminated sites [21].

The key event in metal respiration is the transfer of electrons to the external surface of the cell. Electrons can only travel minute distances (< 10Å), therefore, electron transfer from the outside of the cell to a metal or anode surface must be

accomplished via a series of electron transfer proteins, soluble shuttles, or any combination of the two [22] [23]. An example of a DMRB that utilizes redox active compounds is *Shewanella oneidensis*. This DMRB excretes compounds such as FMN and riboflavin to aid in electron transfer to the electrode [24]. These compounds act by getting reduced by bacterial cytochromes at the membrane, diffuse to the electrode or metal surface, and reduce the acceptor. The shuttles, in their oxidized form, then cycle back to repeat the process. Mediator-dependent dissimilatory metal reduction can be inefficient, especially over longer distances (>1μm), due to diffusion limitations and the degradation of shuttles over time, requiring replenishment. In contrast, bacteria, such as *Geobacter* have evolved the ability to transfer electrons to an insoluble acceptor via direct contact, eliminating the need for a redox active shuttle.

Conductive pili termed "nanowires" have also been described as a way for specialized bacteria to reduce insoluble metals. These pili have been proposed to assist in transfer of electrons from the membrane to the insoluble acceptor, but it is not yet clear if this is due to structural or conductive properties. *G. sulfurreducens* mutants lacking the gene for the key subunit of type IV pili, *pilA*, were unable to produce pili and were unable to reduce insoluble electron acceptors such as Fe(III) and Mn(IV) oxides [25]. When pili are absent from *G. sulfurreducens,* thinner biofilms also result on electrodes, leading to the proposal that pili are responsible for long-range electron transfer [26]. However, when pili are absent the cells also do not agglutinate or form biofilms on glass slides, suggesting that pili are required for cell-cell contact, not necessarily electron

transfer [27]. Studies have also shown that redox-active proteins festoon *Geobacter* pili and are likely directly involved in the propagation of current down the pili [25, 28, 29].

While the mechanism of electron transfer remains under debate, it is clear that *Geobacter sulfurreducens* PCA is a bacterium capable of direct-contact dissimilatory metal reduction, and that *c*-type cytochromes play a key role. Further, *G. sulfurreducens* demonstrates the ability to develop as a biofilm on anodes, with respiration occurring throughout the biofilm via a poorly understood mechanism [30, 31].

***Geobacter sulfurreducens* PCA**

Geobacter species are found in a variety of environments. *G.metallireducens* was first isolated from the Potomac River, and represented the first known example of an organism able to couple complete oxidation of organic compounds to Fe(III) reduction. *G. sulfurreducens* was subsequently isolated from a hydrocarbon-contaminated soil in Oklahoma [32, 33]. The *Geobacter* species are members of the deltaproteobacteria and are Gram-negative facultative anaerobes. A notable feature of *Geobacter* is that they can generate ATP by respiring with insoluble electron acceptors and because of this, they have been implicated as a major source of Fe(III) reduction in the environment when acetate is present [4, 20, 32]. This mechanism allows *G. sulfurreducens* to not only reduce Fe(III) oxides but also precipitate radionuclides such as U(IV). Precipitated heavy metals and radionuclides do not pose as much of a risk to drinking water as their oxidized forms.

The phenotype that gives *G. sulfurreducens* the ability to reduce insoluble acceptors also allows *G. sulfurreducens* to use anodic surfaces. For our studies, graphite electrodes are the sole electron acceptor for respiration [30]. In order to reduce electrodes, *G. sulfurreducens* forms biofilms on the anodic surface and, through direct contact, electron propagation occurs throughout the biofilm to the anode surface. Studies have implicated classes of redox-active proteins, *c*-type cytochromes, to be involved in electron propagation and overall biofilm development [19, 30].

***G. sulfurreducens* Biofilms**

Biofilms are aggregations of microorganisms that grow and develop on a variety of surfaces often aided by the formation of an extracellular matrix. Biofilm development has been proposed to be a developmental process, requiring differential gene expression as cells grow outward from the initial attachment site [12]. Biofilms are far from homogeneous; differences in pH, stress tolerance, and substrate availability throughout the biofilm vary [10]. Therefore, differential gene expression may occur as a result of these zones of heterogeneity.

The environment of a conductive biofilm becomes less homogenous as it develops and cells grow further from an electrode. When the electrons ultimately reduce the anode, they leave behind the protons which must diffuse out of the biofilm. This causes a decrease in pH near the base (close to the electrode) of high current-producing biofilms [34]. Substrate availability could also cause differential expression to occur in biofilms if substrates are utilized by the bacteria before they diffuse to the anode surface.

The accumulation of biomass and the development of a complex structure on the anode also poses a challenge related to electron transfer over long distances. A conductive matrix or specialized structures need to be produced for the cells at the "top" of a current producing biofilm to still respire, and it is likely that the redox proteins needed for long range transfer differ from those involved in interfacial transfer. Therefore, it is hypothesized that, for developing, current producing biofilms, changes in the expression of *c*-type cytochromes take place to facilitate efficient electron transfer throughout the biofilm at different stages [10].

For current propagation through a biofilm to an anode, there needs to be cell-to-cell attachment or cell association with intercellular matrix. Cells need to be anchored together to preserve the structure and function of the biofilm. Cells need to be in contact throughout the biofilm so that electrons produced from metabolism are passed throughout the biofilm and between cells, because electrons cannot travel long distances (< 10 Å) on their own. Second, the biofilm itself has to attach to the anodic surface. The cells at the bottom (closest to the electrode) of the biofilm are in the most direct contact with the surface, therefore, strong adhesion to the surface needs to occur. Finally, there needs to be efficient electron transfer through the entire biofilm to the surface, completing the "circuit" [35]. In order for all this to happen it is likely that different proteins are required according to the phase of biofilm development, possibly at specific times and places in the biofilm. While some research has revealed differential expression of important *G. sulfurreducens* biofilm genes on anodic surfaces, and revealed proteins that appear to be

abundant during current production, to date, there is no work examining the effect of time or distance of gene expression [36, 37].

G. sulfurreducens Cytochromes and Gene Expression in Biofilms

Transcription profiling and proteomics have shown that there are families of proteins that are integral for biofilm structure, development, and current production. Studies have revealed that, along with pili that are strongly involved in attachment and current propagation, cytochromes are involved in electron transfer throughout current-producing biofilms [38]. The genome of *G. sulfurreducens* encodes a large number of known and putative cytochromes, suggesting that different cytochromes are utilized at different times or in different locations in the biofilm, depending on redox or pH conditions [39]. Transcriptional profiling has yielded data showing upregulation of specific cytochrome genes when *G. sulfurreducens* forms current-producing biofilms on anodic surfaces versus using soluble electron acceptors, supporting this hypothesis [36, 40].

For example, *omcS* (GSU_2504), the gene encoding a hexaheme *c*-type cytochrome, has repeatedly been shown to be upregulated during growth with metals and electrodes. This cytochrome was first discovered as one of the most abundant cytochromes sheared from *G. sulfurreducens* cells grown on Mn oxides. This led to the proposal that it is loosely associated with the outer membrane [40]. However, recent immunolabeling has shown that OmcS is associated with the pili and ECM, not the outer membrane [29]. When grown on Fe(III), *omcS* is in higher abundance when compared to

Fe (III) citrate grown cells, and mutants lacking OmcS have the inability to reduce Fe (III) oxides [40]. The transcript for *omcS* has also been shown to be in high abundance when *G. sulfurreducens* colonizes the electrode and produces current in comparison to cells grown with Fe (III) citrate as the electron acceptor [41].

Another cytochrome of interest is OmcZ, an abundant heptaheme cytochrome. OmcZ is important in current production in *G. sulfurreducens* biofilms, which is evident as mutants lacking OmcZ barely produce any detectable current [36, 37]. Microarray analysis has also shown that the abundance of *omcZ* increases when electrodes are electron acceptors when compared to soluble Fe (III) citrate [36]. In addition, a mutant (ΔGSU_1501) defective in production of extracellular polysacchride was recently shown to be unable to anchor OmcZ to the outer surface (Rollefson et al.-Manuscript in review, 2010), and this mutant was also unable to produce current. These results highlight importance of these proteins in current producing biofilms, however, no studies have described where in biofilms these genes are expressed.

Green Fluorescent Protein and Promoter Fusions

Green fluorescent protein (GFP) has been used for over a decade to visualize gene expression and localize proteins within cells. GFP was first isolated from the jellyfish *Aequorea victoria.* When first isolated it was shown to fluoresce without the need for complicated co-factors. The only cofactor needed for fluorescence is oxygen [42]. This is what has made, and still makes GFP so attractive to microbiologists and molecular researchers. The wide use of GFP has led to many different mutations of the protein

resulting in the entire visible spectrum of fluorescent colors. The properties of GFP make it ideal for measuring expression of genes or protein localization in real time and on the single cell level through the use of microscopy and/or fluorescent cell counters. Many researchers want to elucidate the location of proteins within cells and GFP is an attractive option because it is capable of fusions to other proteins. Translation of GFP-fused proteins can be visualized in real time within the cell. When a promoter region of a gene of interest drives the expression of a fluorescent protein, the visualization of fluorescence is correlated to the expression of that gene.

Promoter-reporter (GFP and variants) fusions have been used in transcriptional studies to determine promoter activity. Uri Alon et al. used promoter fusions to fast-folding variants of GFP in order to screen activity of approximately 2000 different promoters (75% of promoters) in *E. coli* K12 [14]. They were able to make a dynamic profile of how these promoters function, both in terms of when the promoters turned on the genes and how strongly the promoters drove transcription. Promoter-reporters can be used to look at gene expression in single or mixed-culture biofilms to visualize biofilm-specific genes. Biofilms are dynamic, changing in response to the microenvironment. Molin et al. wanted to visualize the distribution of growth in a biofilm by pairing a growth rate-regulated promoter (*rrnB*P1) from *E. coli* to an unstable variant of GFP [43].

Addition of specific amino acids to the C-terminus of a fluorescent protein tags the protein for increased degradation by an ATP-dependant protease and significantly shortens the half life of the protein [44]. Unstable GFP degrades more rapidly than GFP without a degradation tag. A cytoplasmic ATP-dependent protease, ClpXP, recognizes

the C-terminal degradation tag and targets the fluorescent protein for rapid degradation. When the half-life of a GFP tagged with the LVA degradation (AANDENYALVA) was measured against a non-tagged GFP in *E. coli* the half-life was significantly shortened. The half-life was reduced from 42 hours for the non-tagged GFP to 74 min for the LVA tagged GFP [44]. This allows for the determination of growth rates of labeled bacteria in biofilms over time [43]. These fluorescent proteins need oxygen to oxidize and fold properly leading to fluorescence. As is the case with *G. sulfurreducens*, many biofilms are anaerobic, or contain anaerobic microenvironments. This poses a challenge for visualizing gene expression when using these fluorescent reporters for promoter-reporter fusions. Although they will fold properly anaerobically and subsequently fluoresce when introduced to oxygen, fluorescence will occur as far as oxygen can permeate the biofilm.

Biofilm studies in which promoter-reporter visualization has been employed have predominantly been interested in the spatial organization of cells within the biofilm. The Newman group fused the promoters of genes for growth and also for metabolism to genes of variants of *gfp*. The gene for *mtrB*, a membrane bound beta-barrel protein that helps coordinate electron transfer under low oxygen or anaerobic conditions was of interest. In the study, and enhanced green fluorescent protein (EGFP) was tagged with a C-terminal degradation tag (AAV) and fused to the promoter of *mtrB* so that patterns of metabolism could be visualized in a developing biofilm. It was suggested that in a biofilm not actively growing, areas of the biofilm that were anaerobic would still be actively metabolizing. The study showed that with the *mtrB-gfp* (AAV) fusion metabolism was occurring in the anaerobic interior of the biofilm [13].

Earlier, it was discussed that *G. sulfurreducens* produces a variety of cytochromes that are necessary for the extracellular transfer of electrons to insoluble substrates. If *Geobacter* biofilms follow a developmental process then it is hypothesized that certain cytochromes are needed at different times and at different locations. The aim of this research was to develop a new tool for visualizing gene expression in *G. sulfurreducens* biofilms. Promoter-reporter fusions were done on the outer membrane cytochromes OmcZ and OmcS. We were interested in visualizing where these omcs were expressed in a developing biofilm on an anodic surface. This was accomplished by coupling the expression of a GFP variant, mCherry, with the promoter of the cytochrome of interest. The mCherry is tagged with a C-terminal degradation sequence (AANDENYALVA) so that it is degraded rapidly, more rapidly than the AAV tag. Visualization can then give insight into the temporal and spatial expression of the cytochrome and be paired with electrochemical data to describe the biofilm.

Materials and Methods

Bacterial strains and culture media. *G. sulfurreducens* strain PCA (ATCC 51573) was kept as liquid culture at 30°C using a vitamin-free anaerobic medium prepared to the following specifications per liter: 0.38 g KCl, 0.2 g NH_4Cl, 0.069 g $NaH_2PO4 \cdot H2O$, 0.04 g $CaCl_2 \cdot 2H_2O$, 0.2 g $MgSO_4 \cdot 7H_2O$, and 10 ml mineral mix; 0.1 g $MnCl_2 \cdot 4H_2O$, 0.3 g $FeSO_4 \cdot 7H_2O$, 0.17 g $CoCl_2 \cdot 6H_2O$, 0.1 g $ZnCl_2$, 0.04 g $CuSO_4 \cdot 5H_2O$, 0.005 g $AlK(SO_4)_2 \cdot 12H_2O$, 0.005 g H_3BO_3, 0.09 g Na_2MoO_4, 0.12 g $NiCl_2$, 0.02 g $NaWO_4 \cdot 2H_2O$, and 0.10 g Na_2SeO_4 added to 1L of double-distilled deionized water. Acetate served as the electron donor at a concentration of 20 mM. The pH was adjusted to pH 6.8, the volume brought to one liter and 2 g/liter $NaHCO_3$ (bicarbonate buffer) was added. The medium was flushed with oxygen-free N_2-CO_2 (80:20 [vol/vol]), sealed with a butyl rubber stopper, and autoclaved [31]. To some of the media Gentamycin was added to a final concentration of 20 μg/mL before anaerobic flushing and autoclaving. *E. coli* strain UQ950 were used for blue/white screening and grown on Luria Broth (LB); 2.5g/L NaCl, 2.5 g/L Trypticase peptones, 5g/L yeast extract, with 20 μg/mL Gentamycin and 50 μL of 20 mg/mL x-gal (5-bromo-4-chloro-3-indolyl- beta-D-galactopyranoside) and grown at 37C. Verified plasmids were transformed into *E. coli* strain WM064 and grown in LB with Gentamycin and 30μm DAP at 37°C. *G. sulfurreducens* transformants were grown on minimal medium plates containing Gentamycin.

Promoter regions: The promoters of two important outer membrane cytochromes (Omcs) were chosen; OmcS (GSU_2504) and OmcZ (GSU_2076). Promoter regions

were predicted from the GSEL database [45]. A region upstream of the predicted start (ATG) of *omcS* containing 400 bases was amplified using the primers 2504 Pro For and 2504 Pro Rev. A region of 400 bases was chosen arbitrarily and it was thought that the necessary promoter elements would be included. A region upstream of the start (ATG) of *omcZ* containing 400 bases was amplified using the primers 2076 Pro For and 2076 Pro Rev. The regions were amplified with the following conditions: 30 cycles of 95°C for 30 sec, 55°C for 1 min, 72°C for 1 min, and a final extension of 72°C for 10min. The fluorescent protein mCherry was amplified from the plasmid p-RSET-B-mCherry with the primers mCherry For and mCherry Rev. A degradation tag was also added to the end of the mCherry to make it unstable using the same forward primer, mCherry For, and the primer mCherry LVA Rev. The regions were amplified with the following conditions: 30 cycles of 95°C for 30 sec, 57°C for 1 min, 72°C for 1.5 min, and a final extension of 72°C for 10min. The promoter regions and mCherry/LVA were digested with BamHI and subsequently ligated together. A 0.8% agarose gel was run and the correctly ligated products identified, excised, and cleaned using a Wizard PCR and Gel cleanup kit. The bands were amplified using the appropriate forward and reverse primers and amplified with the following conditions: 30 cycles of 95°C for 30 sec, 55°C for 1 min, 72°C for 1.5 min, and a final extension of 72°C for 10 min. The primers and their sequences can be found in table 1.

Plasmid. The plasmid pBBR1MCS-5 was initially used as the vector [46]. The gene for mCherry was inserted after the *lac* promoter in pBBR1MCS-5 for constitutive mCherry

expression. The plasmid pRG5Mc, constitutively expressing the fluorescent protein mCherry driven by the *tac-lac* promoter, was obtained from the Lovley lab [37]. To allow for conjugation with mating-strain *E. coli* the Gentamycin resistance cassette and mobilization genes were amplified from pBBR1MCS-5 and inserted into the Spectinomycin cassette of pRG5Mc. Red colonies were picked from a Gentamycin LB plate and the plasmid recovered. The plasmid was named pRG5Mc mob-gent. The mobilization elements, Gentamycin resistance cassette, and multiple cloning site (mob/Gent/MCS5) were amplified from the plasmid pBBR1MCS-5 using the primers Lac/MCS5 For and Mob Rev. The fragment was inserted into the pRG5Mc plasmid with XmnI restriction sites; removing the mCherry fluorescent gene. Transformation into *E. coli* UQ950 cells occurred and colonies that were colorless were verified via PCR with the Lac/MCS5 For and Mob Rev primers for the insert. A verified colony was grown in a 10mL liquid LB culture and a plasmid extraction done using a Quiagen MiniPrep kit. The plasmid was designated pRGMCS5 (fig. 2). OmcZ-mCherry, OmcZ-mCherryLVA, OmcS-mCherry, OmcS-mCherryLVA, and pRGMCS5 were double digested with NEB enzymes PvuI and XbaI. The enzymes were heat killed at 80°C for 20 min and the promoter-reporter fusions ligated into the *lacZ*-α fragment in pRGMCS5. The reactions were allowed to incubate at 16°C overnight. Transformation in *E. coli* UQ950 cells was done with the ligation mixtures and plated on LB with 20 μg/mL Gentamycin and x-gal. After incubation at 37°C, white colonies were picked and verified via PCR with the primers Seq For and Seq Rev. Once a colony was verified it was grown in 10 mL LB and Gentamycin overnight and then a plasmid extraction done with a Qiagen Kit. The

promoter-reporter plasmid construct was then transformed into chemically competent mating strain *E. coli* WM3064. The primers can be found in table 1 and the plasmids in table 2.

Conjugation. *E. coli* WM3064 containing the promoter-reporter fusion plasmid was grown in LB and Gentamycin overnight and washed several times to remove the Gentamycin. Wild-type *G. sulfurreducens* was grown to an OD_{600} of 0.3-0.4 in minimal medium. The cultures were mixed aerobically in a 1:1 ratio and vacuum filtered onto a 0.45µm-pore filter (Millipore). The filter was placed on a vitamin-free minimal plate and placed into a MACS MG500 anaerobic workstation (Don Whitley Scientific Limited, England) containing 5% H_2, 20% CO_2, and 75% N_2 gas. The plates were allowed to incubate overnight. Filters were then suspended in approximately 5 mL growth medium and vortexed to remove cells. The re-suspended culture was plated and colonies selected for on vitamin-free minimal media plates containing Gentamycin. Colonies picked were maintained in liquid minimal medium for studies [47]. Freezer stocks were made of the constructs and stored in 10% DMSO (Dimethyl sulfoxide), a cryoprotectant, at -80°C.

Fluorescent Spectroscopy. *G. sulfurreducens* cultures containing the promoter-reporter plasmid were grown to an OD_{600} of 0.4-0.5 and 1 mL drawn and spun down at 14000 x g for 1 min. The supernatant was poured out and the pellet re-suspended in 400 µL potassium phosphate buffer-Mg/Ca, pH 7, and 200 µL of the culture added to 2 wells of an opaque, fluorescent microtitre plate. The plate was placed in a SpectroMax

spectrophotometer aerobically and read at an excitation of 587 nm and emission of 610 nm for 6 hour with readings taken every 20 min.

Bioreactors. Glassy carbon flags cut into the dimensions 2.1 mm by 0.5 mm by 0.1 mm, were sanded with 1500 grit carbide sandpaper (3M, Minneapolis, MN). Sanded electrodes were sonicated in distilled water for 20 minutes to remove debris. Carbon flags were reused after each experiment after sanding and sonication. Platinum wire was inserted into heat-pulled glass capillary tubes (Kimble, Vineland, NJ) and soldered to copper wires. The polished carbon flags were attached to 0.1 mm Platinum wire with a miniature nylon screw and nut; this ensured electrical contact and designated the working electrode. The resistance of the working electrode was tested and used if the resistivity was below 1 ohm. Counter electrodes were prepared by inserting 0.1mm Pt wire into a heat-pulled glass capillary tube and soldered to copper wire. A salt bridge was created by heat sealing a 3 mm Vycor frit (BioAnalytical Systems, West Layfayette, IN) to a glass capillary tube and fashioned to a 10mL syringe. The working electrode, counter electrode, salt bridge and a gas port made from plastic tubing were inserted into a custom made Teflon lid. The lid contained an O-ring gasket that formed a waterproof seal with the 20mL conical electrochemical cell (BioAnalytical Systems, West Layfayette, IN). The bioreactor was washed with Acetone then 1N NaOH and 1N HCl in alternating intervals. The reactors were rinsed with ethanol, filled with distilled water, and a small magnetic stir bar added. The whole bioreactor was autoclaved. The junction between the lid and the cell was sealed with Parafilm before usage. The salt bridge was filled with 1%

agar containing 0.1M Na_2SO_4. A calomel reference electrode (Fisher Scientific, Pittsburg, PA) was placed on the top of the agar and more 1M Na_2SO_4 added to make sure electrical contact was established. The reactors were placed in a 30C water bath with and connected to humidifiers gassed with sterile N_2-CO_2 (80:20 [vol/vol]). The magnetic stir bars in the reactors were stirred with an external magnet-rotor unit. Sterile minimal medium containing acetate but no fumarate replaced the sterile water in the bioreactor and allowed to purge with N_2-CO_2. Electrochemical techniques were used to be sure of anaerobic conditions by running differential pulse voltammetry (DPV) and cyclic voltammetry on the clean electrodes. Once the DPV and CV showed uniformity and lack of oxygen, the cells were ready for inoculation. Bioreactors were inoculated with 50% (vol/vol) of late log/stationary phase (OD600 of ~0.5) [31].

Electrochemical Techniques. A potentiostat (VMP, Bio-Logic, Knoxville, TN) was connected to the three-electrode bioreactor as described above and controlled with EC-Lab software (EC-Lab v9.41) The techniques CV, DPV, and chronoamperometry (CA) were used. DPV and CV were run in succession at the beginning of the program. The parameters for DPV were as follows: *E*initial (*Ei*) = –0.558 V versus SHE and *E*final (*Ef*) = 0.242 V versus SHE; pulse height, 50 mV; pulse width, 300 ms; step height, 2 mV; step time, 500 ms; scan rate, 4 mV/s; current averaged over the last 80% of the step (1 s, 12 points); accumulation time, 5 s. The parameters for CV were as follows: equilibrium time, 5 s; scan rate, 1 mV/s; *Ei* = –0.558 V versus SHE; *Ef* = 0.242 V versus SHE; current averaged over the whole step (1 s, 10 points). A CA was then set to run

continuously for 72 hours. The CA parameters were *E*applied (*E*) = 0.242 V versus SHE. Current was monitored and the cells stopped with the desired current reached [31].

Confocal Microscopy. At the appropriate current, electrodes were taken out and placed in 100mM phosphate buffer Mg/Ca mix containing 0.1% of 5mM Syto9 in DMSO (Invitrogen Corp., Carlsbad, CA). The electrode was allowed to oxygenate in the dark and at 4C for approximately 1-1.5 hours and then taken out and placed in clean phosphate buffer to wash away the residual Syto9. A Nikon C1 spectral imaging confocal microscope (Nikon, Japan) with a 60XW (water immersion) lens was used to image the developed biofilm. The electrode was placed biofilm side down on a drop of *Bac*Light mounting oil (Invitrogen Corp., Carlsbad, CA) on a 24X50mm glass coverslip (Fisher Scientific). Laser wavelengths of 488 nm and 561 nm were used to excite Syto9 and mCherryLVA respectively. Z stacking was done to produce a cross section of the biofilms with a stack size of 30 μM. Images were rendered in the EZ-C1 Nikon Software Package and analyzed. In order to be able to clearly visualize mCherry expression the images were autocorrected so that the fluorescent intensity maximized.

Table 1. Primers and sequences used for PCR amplifications.

Primer	Target	Restriction Site	Sequence
2504 Pro For	OmcS promoter region	PvuI	ATTATTCGATCGGCAGTTCAAGTTCATC
2504 Pro Rev		BamHI	GGTACCCGGGGATCCTCTAGCATTTCCT CCATTTTGGTTG
2076 Pro For	OmcZ promoter region	PvuI	ATTATTCGATCGGCTGAACGTTAAAATG
2076 Pro Rev		BamHI	GGTACCCGGGGATCCTCTAGTCCTTTCTG CTCCTTTCTTG
mCherry For	mCherry	BamHI	GGTGGACAGCAAATGGGTCG
mCherry Rev		XbaI	CTCCGGTCTAGATTACTTGTACAGCT
mCherry LVA Rev	mCherry with LVA	XbaI	TAATTCTAGATCAGGCCACCAGGGCGTAG TTCTCGTCGTTGGCGGCCTTGTACAGCTC G TCCATGC
Lac/MCS5 For	Mob/Gent/MCS5 from pBBR1MCS5	XmnI	ACCAGAAGCCGTTCAGTCGGCCTATTGGT T AAA
Mob Rev		XmnI	TAAGAATAATTTCCTGCGCGGTCGCTGCG C GAG
Seq For	Used for PCR verification and sequencing the MCS5 region of pBBR1MCS5		AGTCGGCCTATTGGTTAAA
Seq Rev			GGAATTGTGAGCGGATAAC

Table 2. Strains and plasmids used for this study.

Strain or Plasmid	Characteristics	Reference
Geobacter sulfurreducens PCA	Isolated from hydrocarbon contaminated soil	[4]
Escherichia coli UQ950	*E. coli* DH5α host for cloning and blue/white screening	[48]
E. coli WM3064	DAP auxotroph used for conjugal mating with *G. sulfurreducens*	[48]
Plasmids		
pRSET-B-mCherry	A plasmid containing the fluorescent protein mCherry	[49]
pRG5Mc	Constitutively expressed mCherry by the *tac-lac* promoter in *G. sulfurreducens*	[34]
pBBR1MCS-5	A broad range host vector used in *G. sulfurreducens*.	[50]
pRG5Mc-mob/gent	Constitutively expressed mCherry by the *tac-lac* promoter with the mob/gent from pBBR1MCS-5	This study
plac mCherry-pBBR1MCS-5	Constitutively expressed mCherry by the *lac* promoter in pBBR1MCS-5	This study
pRGMCS5	pRG5Mc with *tac-lac* mCherry replaced with mob-gent-MCS5 from pBBR1MCS5	This study
pOmcS-pRGMCS5	*omcS* promoter in pRGMCS5	This study

pOmcS mCherry-pRGMCS5	*omcS* promoter driving the expression of mCherry in pRGMCS5	This study
pOmcS mCherryLVA-pRGMCS5	*omcS* promoter driving the expression of mCherryLVA in pRGMCS5	This study
pOmcZ-pRGMCS5	*omcZ* promoter in pRGMCS5	This study
pOmcZ mCherry-pRGMCS5	*omcZ* promoter driving the expression of mCherry in pRGMCS5	This study
pOmcZ mCherryLVA-pRGMCS5	*omcZ* promoter driving the expression of mCherryLVA in pRGMCS5	This study

Plasmid Construction

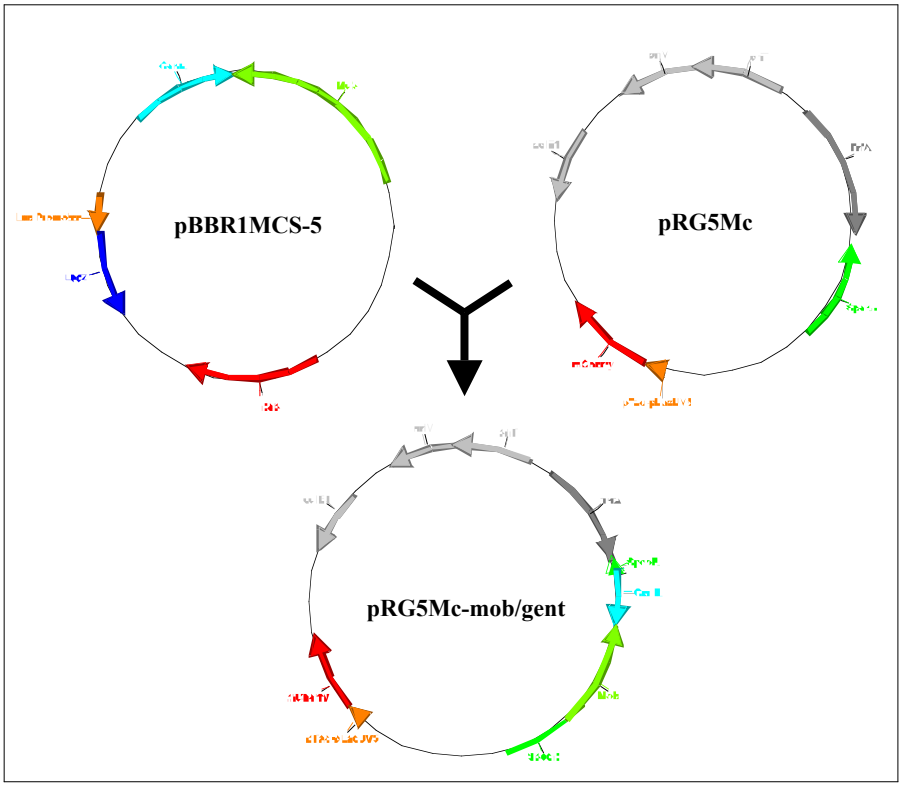

Figure 1-The construction of pRG5Mc mob-gent. The mob-gent region was amplified from pBBR1MCS5 and ligated into the XmnI site within the Spectinomycin resistance cassette.

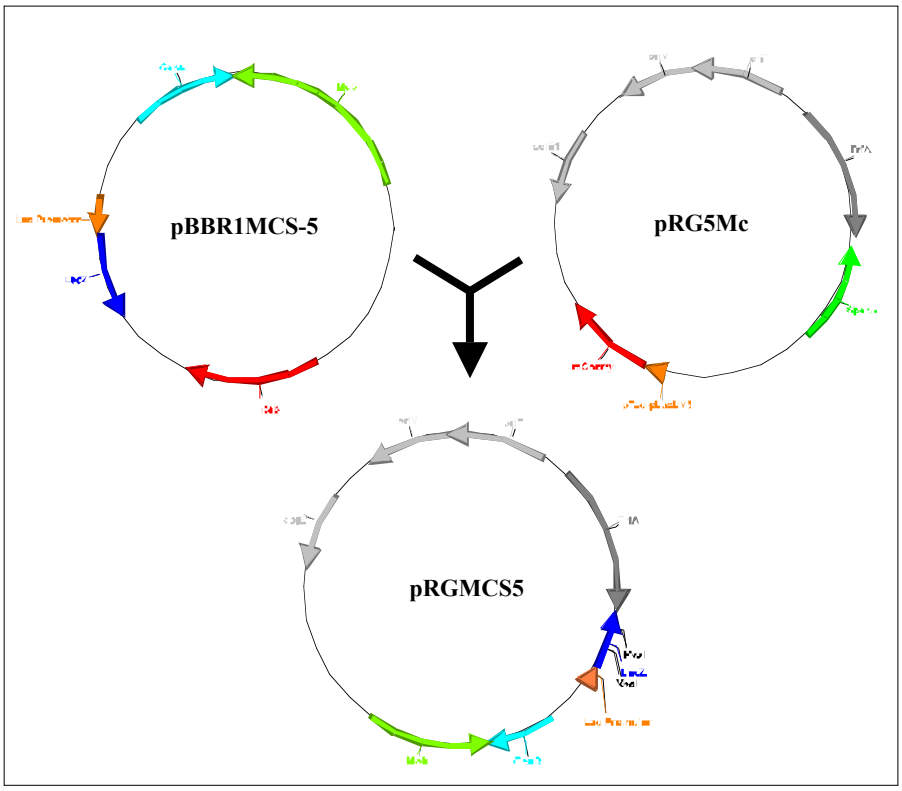

Figure 2-The construction of pRGMCS5. The mob-gent-pLac-LacZ alpha and MCS of pBBR1MCS5 were amplified and ligated into pRG5Mc removing the pTac-LacUV5 mCherry and Spectinomycin resistance cassette. Colonies were screened for the absence of mCherry, LacZ activity, and Gentamyacin resistance

Results

Bioinformatics: The sequences of the genes for the *c*-type cytochromes of interest (*omcZ* and *omcS*) were explored using bioinformatics. The annotated genome of *Geobacter sulfurreducens* was available from the GSEL database hosted at NCBI [45]. To capture the total promoter region, a total of 400 bases were chosen directly upstream of *omcS* (GSU_2504), the first gene in the operon. The region was designated pOmcS. Similarly, the gene for *omcZ* (GSU_2076) was annotated and described by the GSEL database. As with the *omcS* promoter region, 400 bases were amplified upstream from the start of *omcZ* (pOmcZ). To verify the organization of the operons, IGB 6.2.2 was used and the regions confirmed using transcriptional start site information [51]. These regions were amplified and fused to mCherry, with or without the protease recognition tag (LVA) with restriction enzymes. They were inserted into broad-range plasmid pBBR1MCS-5 [46] initially and then into pRGMCS5 [34], a modified plasmid containing the replicon of pRG5Mc . The inserts in pRGMCS5 became the working plasmids for the project.

Promoter-reporters in pBBR1MCS-5: The plasmid pBBR1MCS-5 is commonly used as an expression vector in *G. sulfurreducens*. However, slowed growth and a potentially weak promoter (*p*lac) warranted investigation into a new vector and stronger promoters to drive constitutive expression of mCherry. To determine if mCherry expression could occur in *G. sulfurreducens*, mCherry was inserted after the *lac* promoter in pBBR1MCS-5 (p*lac* mCherry pBBR1MCS-5). No mCherry fluorescence was detected in *G. sulfurreducens* containing p*lac* mCherry pBBR1MCS-5 (data not shown). Growth of *G.*

sulfurreducens containing p*lac* mCherry pBBR1MCS-5 in liquid culture was comparable to wild type (data not shown). Growth of *G. sulfurreducens* containing pOmcS mCherryLVA-pBBR1MCS-5 and with pOmcZ mCherryLVA-pBBR1MCS-5 was also comparable to wild type in liquid culture (data not shown). However, when grown on graphite electrodes, the growth of *G. sulfurreducens* containing any of the promoter-reporter constructs was slow compared to wild type. Figure 3 shows a comparison of *G. sulfurreducens* containing p*lac* mCherry-pBBR1MCS-5 (Old) to *G. sulfurreducens* containing pRG5Mc mob-gent (New) on graphite electrodes showcasing the better growth of *G. sulfurreducens* containing the new constitutive mCherry plasmid.

These results led to construction of the new working plasmid, pRGMCS5 (a modified version of pRG5Mc and pBBR1MCS-5). When *G. sulfurreducens* containing pOmcZ mCherryLVA-pBBR1MCS-5 and *G. sulfurreducens* containing pOmcZ mCherryLVA-pRGMCS5 were compared on electrodes, *G. sulfurreducens* containing pOmcZ mCherryLVA-pRGMCS-5 grew faster and achieved higher current density, similar to what was observed in the constitutive construct (Fig 4). The plasmid pRGMCS5 was then chosen to be the working vector because of apparent better growth on the electrodes.

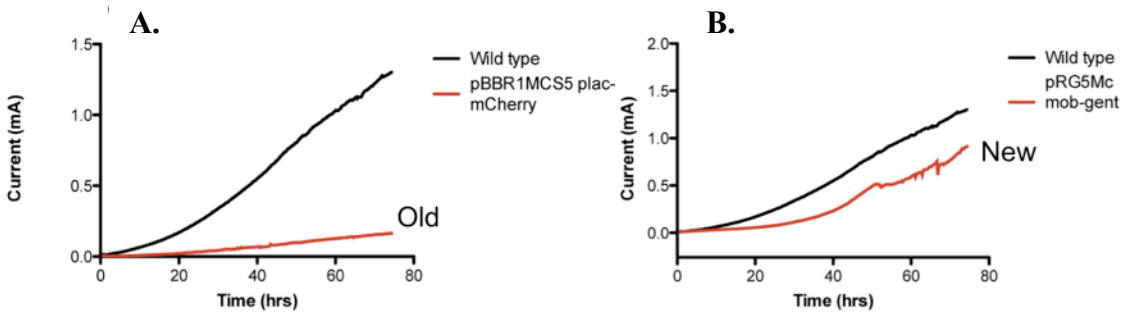

Figure 3-Comparison of *G. sulfurreducens* containing p*lac* mCherry-pBBR1MCS-5 (A) to *G. sulfurreducens* containing pGR5Mc mob-gent (B). The *G. sulfurreducens* containing pRG5Mc mob-gent (New) grew significantly faster than the *G. sulfurreducens* containing p*lac* mCherry-pBBR1MCS-5 (Old).

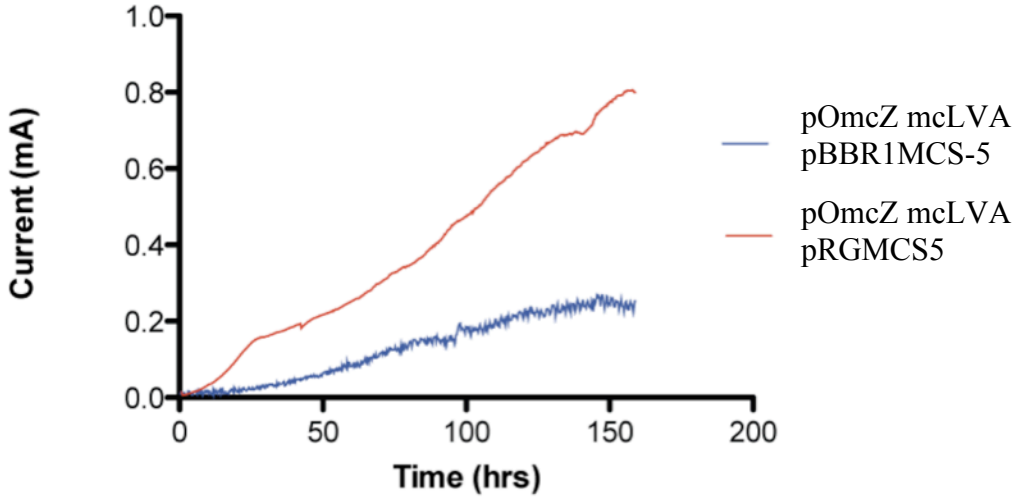

Figure 4-Comparison of *G. sulfurreducens* containing pOmcZ mCherryLVA-pBBR1MCS-5 (blue line) and *G. sulfurreducens* containing pOmcZ mCherryLVA-pRGMCS5 (red line). *G. sulfurreducens* containing pOmcZ mCherryLVA-pRGMCS5 grows faster and produces more current on the electrode than the other construct in *G. sulfurreducens*.

Promoter-reporters in pRGMCS5: The kinetics of mCherry oxidation and fluorescence in *G. sulfurreducens* liquid cultures was studied. After reaching an OD_{600} of approximately 0.45 in liquid medium the *G. sulfurreducens* containing pRG5Mc mob-gent developed maximal fluorescence after approximately 4 hours of oxygen exposure (n=3). The maximum fluorescence (ex. 587 and em. 610) was approximately 250 RFU per OD unit (Fig 5). Attempts to assay the fluorescence of the mCherry modified with the protease recognition sequence (LVA) in *G. sulfurreducens* proved unsuccessful (data not shown), as stable transformants harboring this construct could not be obtained.

G. sulfurreducens containing the pRG5Mc-mob/gent plasmid was grown on the electrode and, when a suitable current reached (1.5 mA), allowed to oxygenate in phosphate buffer (pH 7.0) in order to verify that the visualization of mCherry fluorescence would be possible via confocal microscopy (Fig. 6). Once the ability to visualize mCherry expression in a *G. sulfurreducens* biofilm was shown, *G. sulfurreducens* containing the promoter-reporter constructs were assayed for fluorescence after growth in liquid medium (Fig 7). The fluorescence of the cells containing the promoter-reporter constructs had similar fluorescence to wild type.

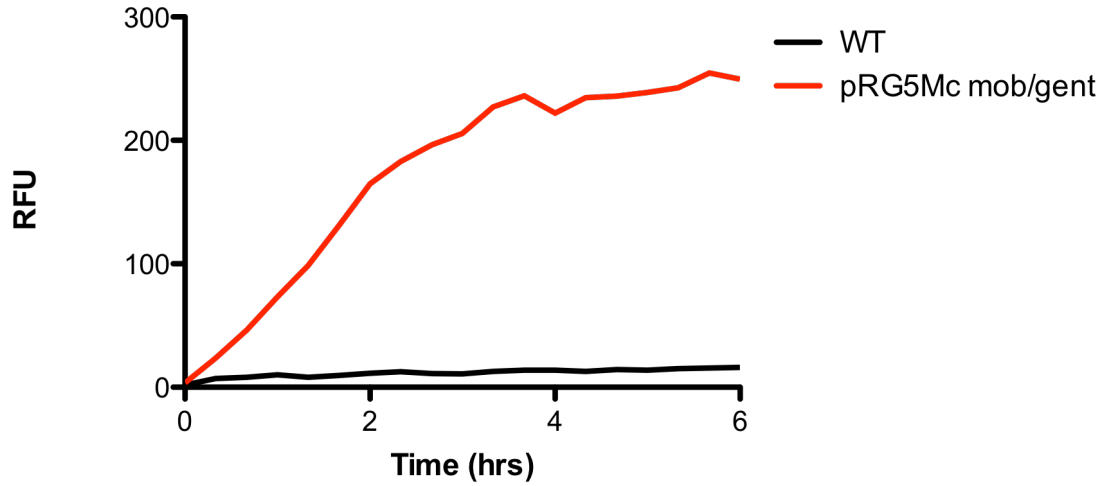

Figure 5- Time needed for total fluorescence of constitutive mCherry (pRG5Mc) in *G. sulfurreducens* as compared to WT in liquid media. Each line represents the mean of three replicates.

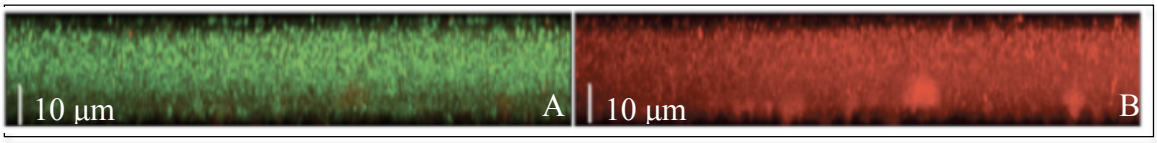

Figure 6-*G. sulfurreducens* containing pRG5Mc mob-gent for constitutive expression of mCherry driven by the p*tac-lac* promoter. The biofilm was allowed to reach a current of 1.5 mA on the electrode and then placed in phosphate buffer at 4°C for 1 hour to oxygenate. The biofilm was stained with Syto9. The left side (A) shows the total biomass in green. The right side (B) represents mCherry expression.

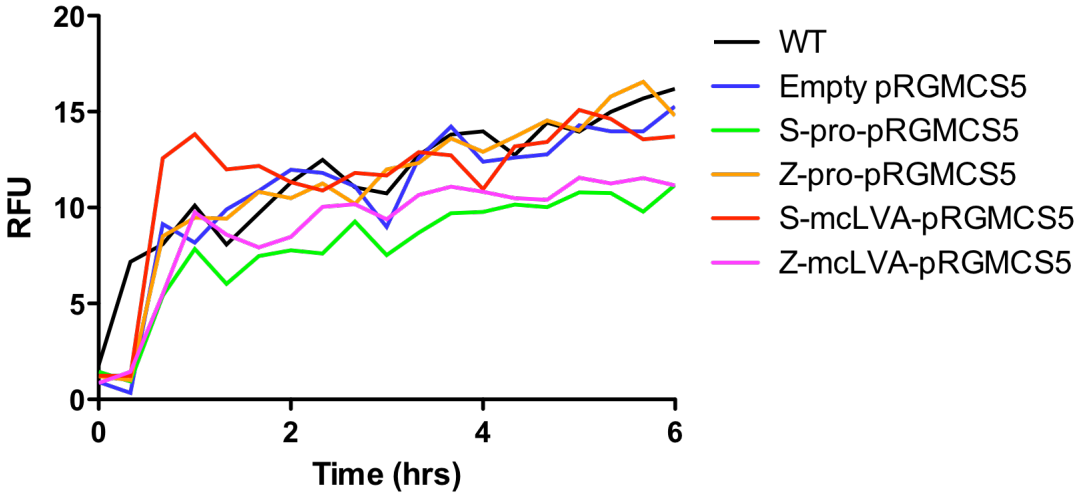

Figure 7- Fluorescence of *G. sulfurreducens* containing versions of the promoter-reporter constructs in liquid medium. Each line represents the mean of three replicates.

Growth curves were performed on *G. sulfurreducens* containing the *omcS* promoter-reporter constructs and compared to wild type growth in liquid medium. Representative growth curves are shown in Figure 8. Growth rates were calculated from exponential growth phase (Table 3). The constitutive expression of mCherry did not reduce growth rate more than 15%. All promoter-reporter constructs caused *G. sulfurreducens* to produce less current than wild type *G. sulfurreducens* on the electrodes. To test if slow growth was due to the promoter or mCherry expression, *G. sulfurreducens* containing the pOmcS constructs were compared to *G. sulfurreducens* containing the empty vector pRGMCS5. While cells containing the vector grew slower on electrodes, the addition of the pOmcS or pOmcZ mCherry vectors didn't change the growth on the electrode significantly (Fig. 9).

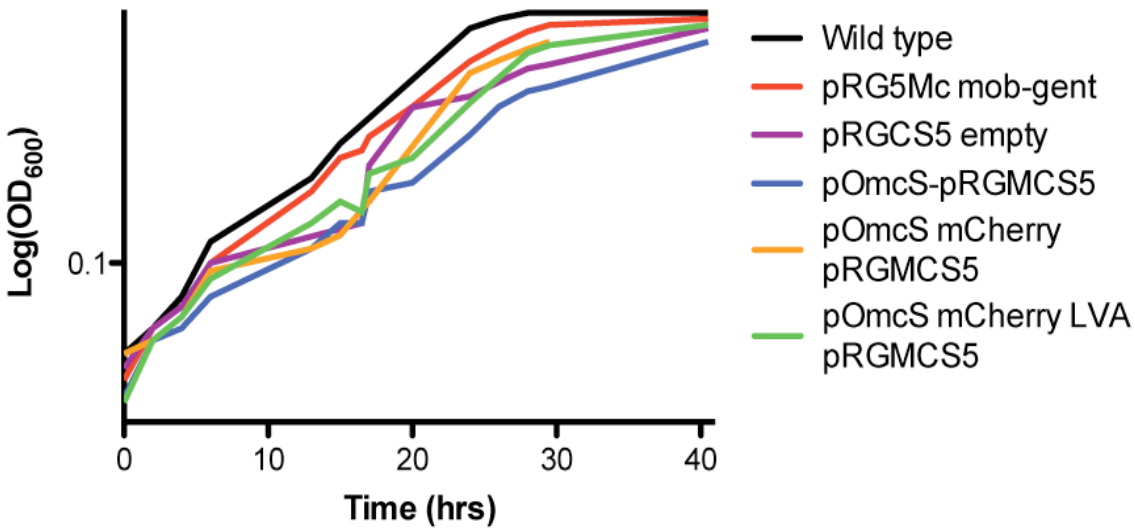

Figure 8-Growth curves comparing *omcS* promoter-reporter constructs in *Geobacter sulfurreducens* and WT.

Table 3-Relative growth rates of *G. sulfurreducens* containing the variants of the *omcS* promoter-reporter constructs in liquid medium.

G. sulfurreducens	μ (hrs $^{-1}$)
Wild type	0.048
pRG5Mc mob-gent	0.041
pRGCS5 empty	0.046
pOmcS-pRGMCS5	0.036
pOmcS mCherry pRGMCS5	0.035
pOmcS mCherry LVA-pRGMCS5	0.038

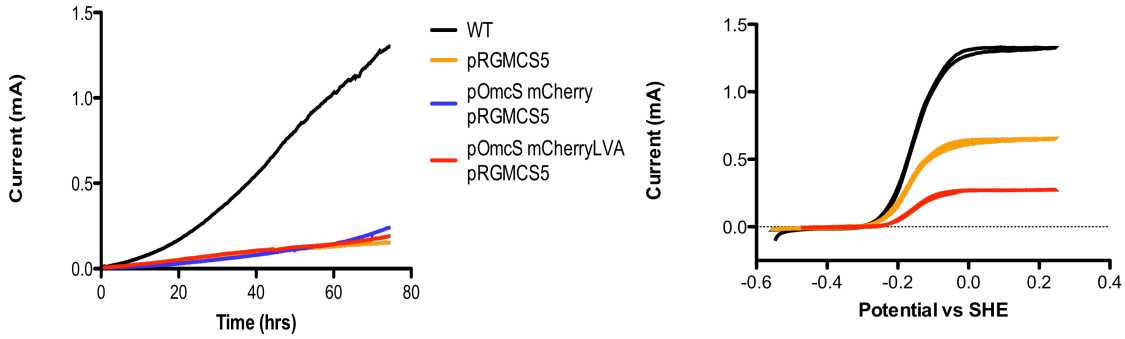

Figure 9- *G. sulfurreducens* containing the pOmcS constructs were compared to *G. sulfurreducens* containing the empty vector pRGMCS5. Current vs. time on the left-hand side reveals that *G. sulfurreducens* containing the empty vector and the pOmcS constructs grow comparatively on the graphite electrode. The current versus potential (right-hand graph) shows the catalytic properties of the biofilms on the electrodes.

Figure 10 shows the current produced by replicates of *G. sulfurreducens* containing pOmcS mCherryLVA-pRGMCS5 on graphite electrodes. The black arrows indicate where the electrodes were harvested and imaged. The electrodes were harvested at ~130, 350, 630, and 800 µA. Previous replicates done of *G. sulfurreducens* containing the same construct yielded the same current productions (data not shown). After being placed in phosphate buffer (pH 7.0), allowed to oxygenate for 1 hour, and stained with Syto9 the biofilms were imaged. Figure 11 show the accumulated biomass of *G. sulfurreducens* containing pOmcS mCherryLVA pRGMCS5 at 135 µA, 350 µA, 650 µA, and ~800µA.

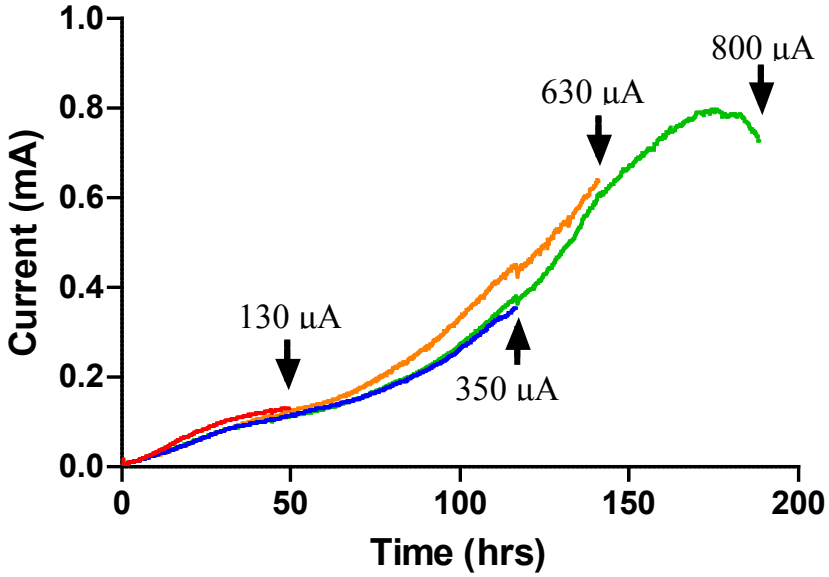

Figure 10-Current vs. time (CA) graph of OmcS mcLVA pRGMCS5. Black arrows indicate the harvesting and imaging of the electrode. The electrodes were harvested at ~130, 350, 630, and 800 µA.

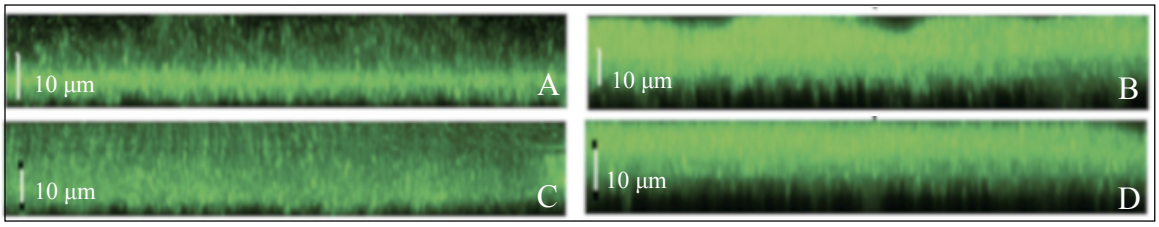

Figure 11- Accumulated biomass of *G. sulfurreducens* containing pOmcS mCherryLVA pRGMCS5 at 135 µA (A), 350 µA (B), 650 µA (C), and ~800µA (D).

In addition to the current series of *G. sulfurreducens* continaing the pOmcS constructs, images of wild type biofilms were obtained for comparison. A wild type *G. sulfurreducens* biofilm was treated as stated above, and imaged after producing approximately 130µA of current (Fig 12). Autofluorescence was noticed in the red

spectrum when imaging. Therefore, the gain for the 568nm laser (red) was set to 6, in hopes to eliminate most of the autofluorescence. This was the setting used throughout for all biofilm imaging. *G. sulfurreducens* containing the empty vector, pRGMCS5 was also grown on a graphite electrode and imaged (Fig 13).

Autofluorescence appears towards the bottom of the *G. sulfurreducens* biofilm containing the empty vector. *G. sulfurreducens* containing pOmcS mCherry-pRGMCS5 was imaged and, although red fluorescence appears throughout, a band of red fluorescence was seen at the bottom of the biofilm (Fig. 14). Extreme caution was used when describing red fluorescence, making it difficult to conclude the expression of mCherry. The current series of *G. sulfurreducens* containing pOmcS mCherryLVA-pRGMCS5 was imaged after the appropriate current was reached (Fig. 15).

It was hypothesized that the overpowering autofluorescence seen is due to the limited oxygenation time (1 hour). Therefore, *G. sulfurreducens* pOmcS mCherryLVA-pRGMCS5 was allowed to oxygenate for 3 hours instead of 1 hour (Fig 16). Figure 17 is a top-down view of *G. sulfurreducens* containing pOmcS mCherryLVA-pRGMCS5 allowed to oxygenate for 3 hours. It appears the longer oxygenation time allows for the mCherry fluorescence to be brighter than the autofluorescence.

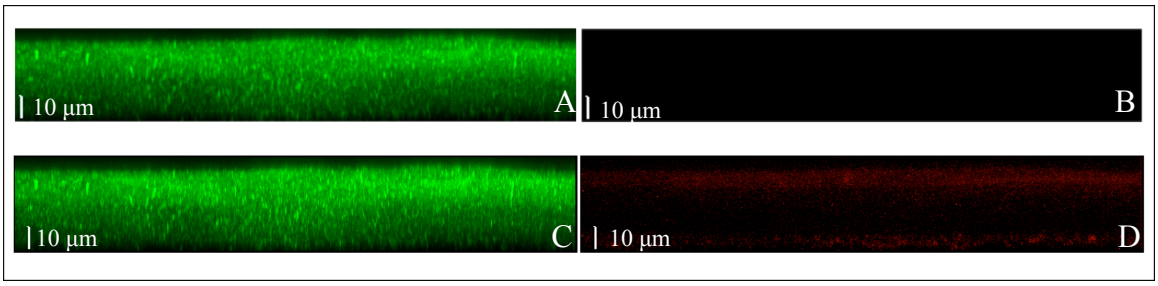

Figure 12-Wild type *G. sulfurreducens* biofilm grown on a graphite electrode imaged at 130 µA, allowed to oxygenate for 1 hour at 4°C, and stained with Syto9 (A) and viewed with only the red (561nm) filter (B); both unprocessed. An image of the same biofilm stained with Syto9 (C) and then the red (561nm) filter (D) was processed with the imaging software to reveal autofluorescence. The scale bar represents 10 µm.

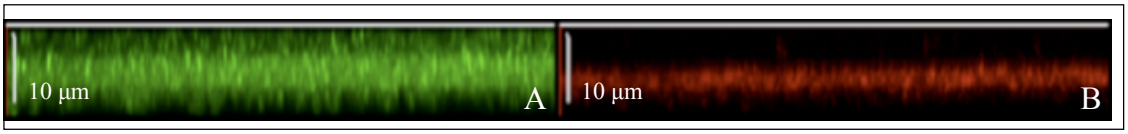

Figure 13-Empty vector, pRGMCS5, in *G. sulfurreducens* grown on a graphite electrode, allowed to oxygenate for 1 hour at 4°C, and stained with Syto9 (A) then viewed using only the red (561nm) filter (B). Scale bar represents 10 µm.

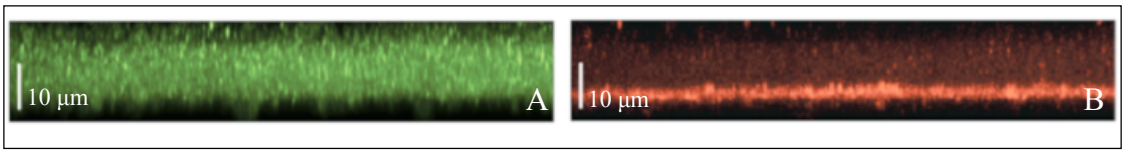

Figure 14- *G. sulfurreducens* containing pOmcS mCherry-pRGMCS5 was allowed to oxygenate for 1 hour at 4°C, imaged, and although fluorescent throughout, the pattern of a band of red fluorescence at the bottom remains. Scale bar represents 10 µm.

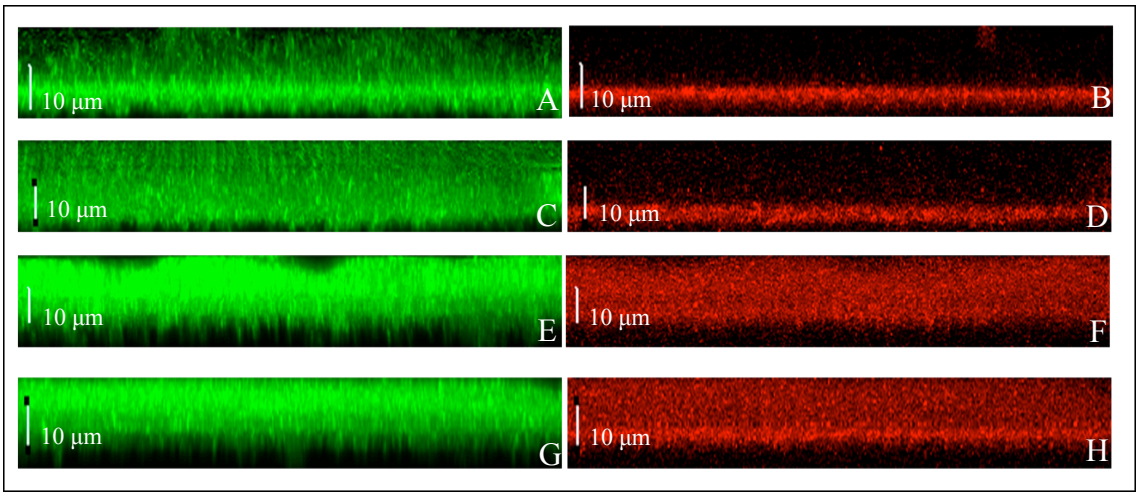

Figure 15-The effect of 1 hour oxygenation vs. 3 hours: the construct for the OmcS promoter driving the expression of mCherryLVA (OmcS mcLVA) pRGMCS5 in *G. sulfurreducens* grown on a graphite electrode and harvested at arbitrary currents. Biofilms were allowed to oxygenate for approximately 1 hour at 4ºC. At 135 µA the biofilm was stained with Syto9 and imaged (A) and then with the red (561nm) filter (B). At 350 µA the biofilm was stained with Syto9 (C) and then viewed with the red filter only (D). The biofilm was harvested at 650 µA and stained with Syto9 (E) then viewed with the red filter (F). Finally, the biofilm was imaged at ~800 µA with Syto9 (G) and then with the red filter (H). Scale bars represent 10 µm.

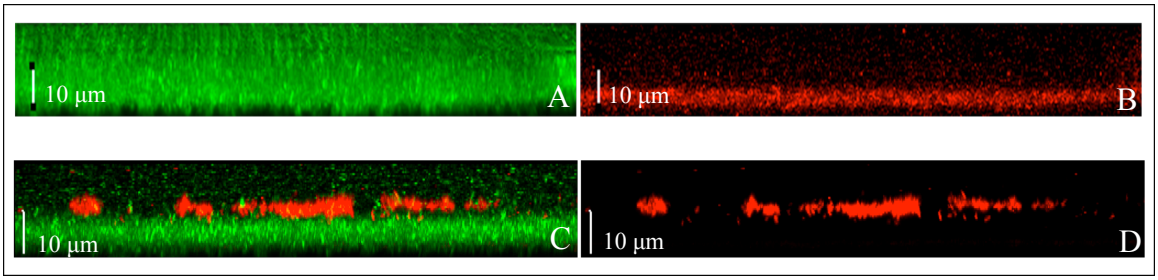

Figure 16- The effect of 3 hour oxygenation vs. 1 hour: the OmcS mCherryLVA construct (OmcS mcLVA) pRGMCS5 in *G. sulfurreducens* grown on a graphite electrode. Comparing the biofilm oxygenated for 1 hour at 4ºC stained with Syto9 (A) and with only the red (561nm) filter (B), autocorrected for brightness, to a biofilm oxygenated for 3 hours at 4ºC and stained with Syto9 (C) and with the red filter (D). The longer oxygenated biofilm did not need auto correction to visualize fluorescence. Biofilms were grown to the same current and the scale bars represent 10 µm.

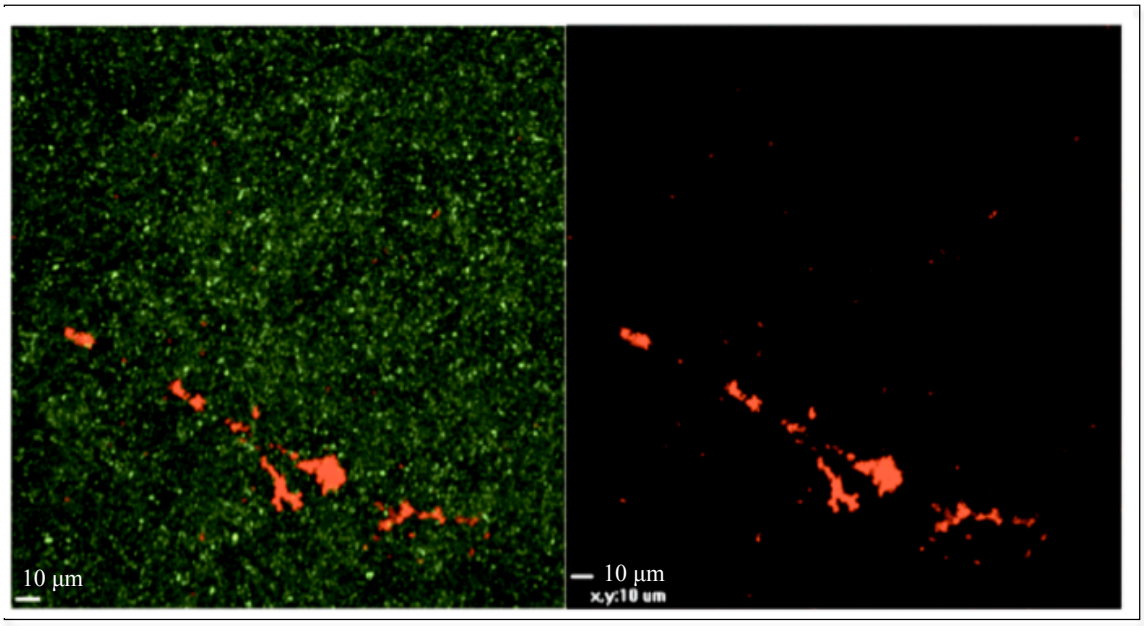

Figure 17- Top-down view of *G. sulfurreducens* containing pOmcS mCherryLVA-pRGMCS5 grown on a graphite electrode. The left panel represents total biomass stained with Syto9 and mCherry expression. The right panel represents only mCherry fluorescence. Biofilms were allowed to oxygenate in phosphate buffer for 3 hours. Scale bars are 10 µm.

The promoter for OmcZ, pOmcZ, was also studied. *G. sulfurreducens* containing pOmcZ variants were grown in liquid medium and their growth measured (Fig. 18). Relative growth rates were calculated, as before, and shown in Table 4. As a comparison, *G. sulfurreducens* containing the pOmcZ variants were compared to wild type on the electrodes, with slower growth occurring (Fig 19). The current series for OmcZmcLVA pRGMCS5 is shown in figure 20. The black arrows indicate the current reached when the electrodes were harvested and imaged. Replicates of the currents reached show similar growth of *G. sulfurreducens* containing pOmcZ mCherryLVA-pRGMCS5 (data not shown).

Again, the images seem to contain a strong band of red fluorescence at the bottom of the biofilm. To reduce the rendering of autofluorescence, the biofilm was allowed to

oxygenate for 3 hours instead of 1 hour (fig 22). A top-down view of *G. sulfurreducens* containing pOmcZ mCherryLVA-pRGMCS5 shows mCherry fluorescence after 3 hours. The left panel shows total biomass and mCherry fluorescence and the right showing mCherry fluorescence (fig. 23)

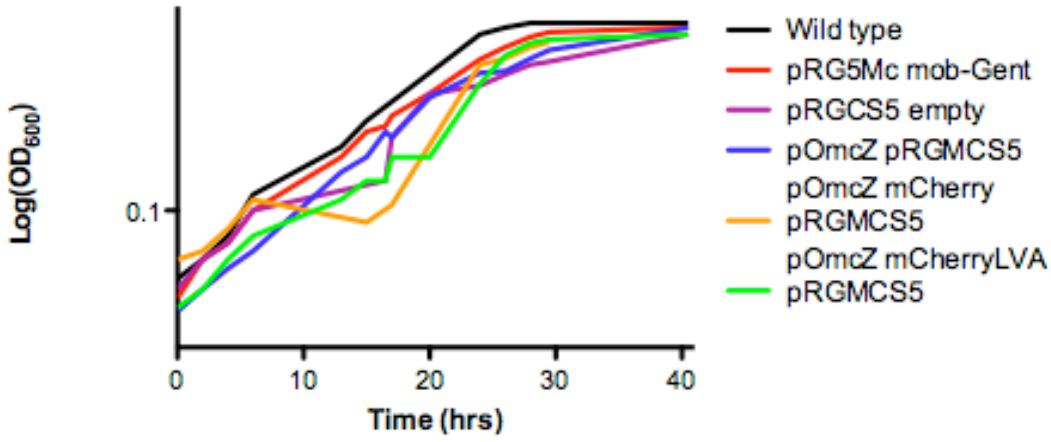

Figure 18-Growth curves of *G. sulfurreducens* containing variants of pOmcZ in liquid medium.

Table 4-Relative growth rates of *G. sulfurreducens* containing variants of pOmcZ

G. sulfurreducens	μ (hrs $^{-1}$)
Wild type	0.034
pRG5Mc mob-Gent	0.032
pRGCS5 empty	0.032
pOmcZ pRGMCS5	0.033
pOmcZ mCherry pRGMCS5	0.029
pOmcZ mCherryLVA-pRGMCS5	0.032

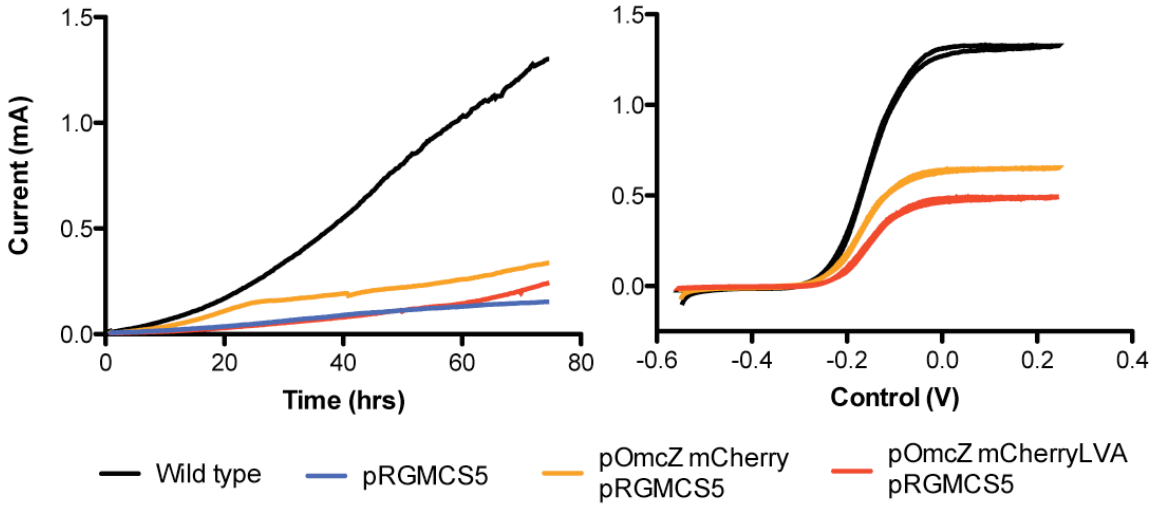

Figure 19-*G. sulfurreducens* containing the pOmcZ variants compared to wild type on graphite electrodes. Again, the promoter-reporter constructs in *G. sulfurreducens* grew slower and produced less overall current than wild type.

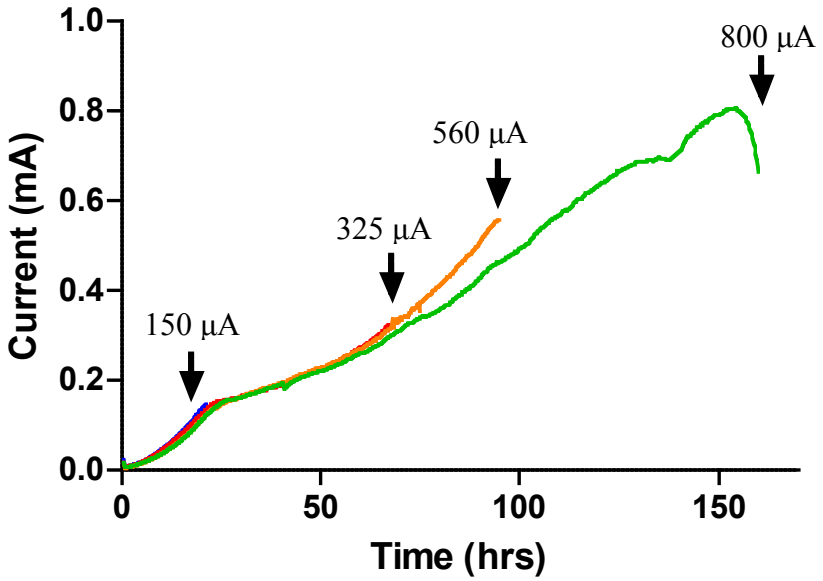

Figure 20-Current vs. time graph of *G. sulfurreducens* containing pOmcZ mCherryLVA-pRGMCS5. The black arrows indicate the harvesting and imaging of the electrode.

Confocal images were taken at 150µA, 325µA, 560µA, and ~800µA as seen in Figure 21.

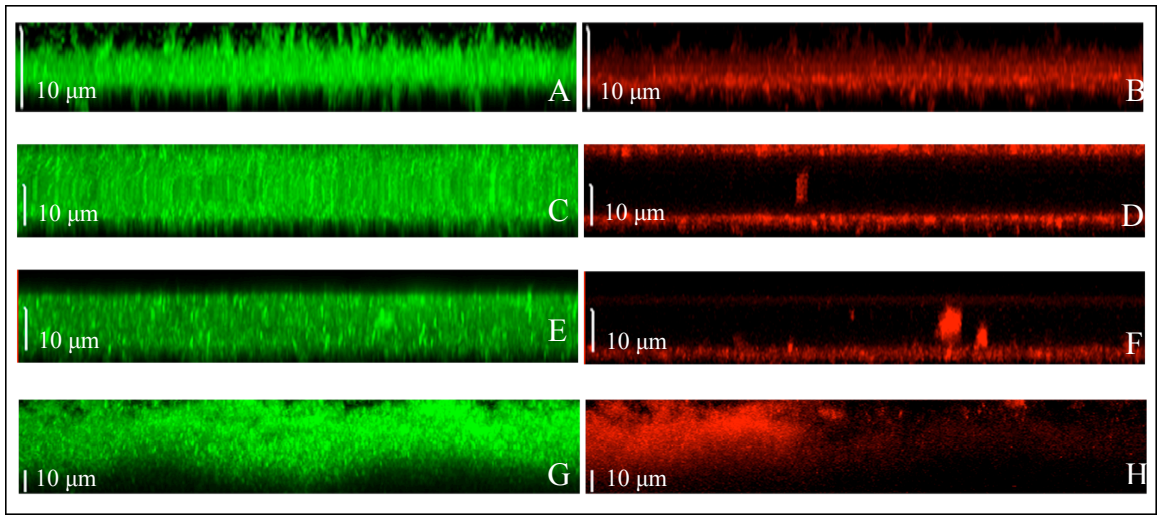

Figure 21- The construct for the OmcZ promoter driving the expression of mCherryLVA (OmcZ mcLVA) pRGMCS5 in *G. sulfurreducens* grown on a carbon electrode and harvested at arbitrary currents. Biofilms were allowed to oxygenate for approximately 1 hour at 4ºC. At 150 µA the biofilm was stained with Syto9 and imaged (A) and then with the red (561nm) filter (B). At 325 µA the biofilm was stained with Syto9 (C) and then viewed with the red filter only (D). The biofilm was harvested at 560 µA and stained with Syto9 (E) then viewed with the red filter (F). Finally, the biofilm was imaged at ~800 µA with Syto9 (G) and then with the red filter (H). Scale bars represent 10 µm.

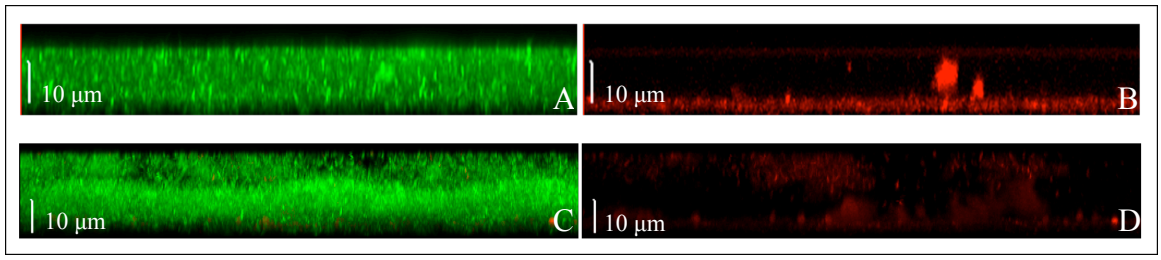

Figure 22-The OmcZ mCherryLVA construct (OmcZ mcLVA) pRGMCS5 in *G. sulfurreducens* grown on a carbon electrode. Comparing the biofilm grown to 560 µA and oxygenated for 1 hour at 4ºC stained with Syto9 (A) and with only the red (561nm) filter (B) to a biofilm grown to 490 µA oxygenated for 3 hours at 4ºC and stained with Syto9 (C) and with the red filter (D). The longer oxygenated biofilm, when rendered, did not show auto fluorescence. Biofilms were grown to roughly the same current and the scale bars represent 10 µm.

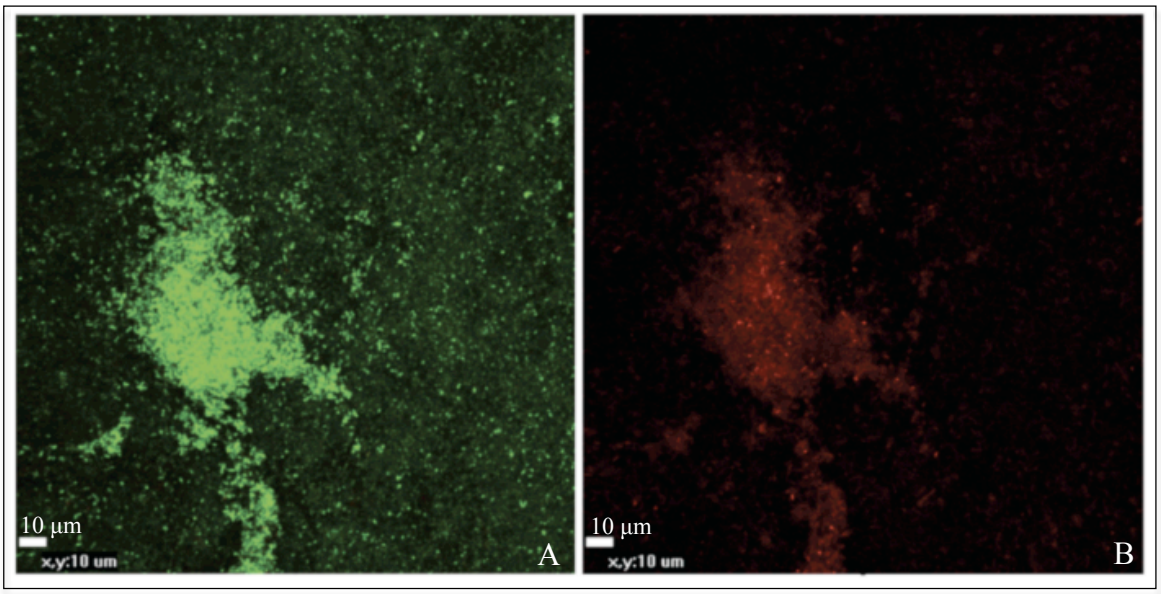

Figure 23- A top-down view of *G. sulfurreducens* containing pOmcZ mCherryLVA-pRGMCS5 shows mCherry fluorescence after 3 hours. The left panel shows total biomass stained with Syto9 and mCherry fluorescence and the right showing mCherry fluorescence. The biofilms were allowed to oxygenate in phosphate buffer for 3 hours. Scale bars represent 10 µm.

Discussion

The goal of this research was to develop a way to visualize gene expression in *G. sulfurreducens* biofilms. Previous studies have tried to describe gene expression through the use of transcriptomics of developing biofilms [36]. The gene for *omcS* was of interest because it encodes an abundant hexaheme *c*-type cytochrome that is proven to be important in Fe (III) oxide reduction and current production of *G. sulfurreducens* biofilms on graphite electrodes [40, 52]. The gene for *omcS* (GSU_2504) is annotated as being the leading gene of an operon, which also includes the gene for *omcT* downstream of *omcS*. It was assumed that by taking a 400 base pair fragment upstream of the gene the promoter region would be captured along with the necessary transcriptional elements. Alon et al. used a similar method of choosing promoter regions for transcriptional studies by choosing ~500 bases upstream of hypothesized *E. coli* promoters [14]. The same was done for the *omcZ* promoter. The gene for *omcZ* is in an operon by itself and transcribed monocistronically. A region of 400 bases upstream of *omcZ* was amplified assuming all the transcriptional elements would be captured.

Initially, the vector pBBR1MCS-5 was used to carry the promoter-reporter constructs. The gene for mCherry was inserted after the p*lac* in pBBR1MCS5. This promoter was thought to drive constitutive expression in *G. sulfurreducens*. Liquid cultures were grown of *G. sulfurreducens* containing p*lac* mCherry-pBBR1MCS-5 and assayed for red fluorescence. No fluorescence was observed in these cultures. This caused us to search for a different constitutive promoter to drive the expression of mCherry. Although *G. sulfurreducens* containing constructs in pBBR1MCS-5 grew

similar to wild type in liquid culture, it was observed that they grew much slower than wild type on graphite electrodes (Fig 3). When the plasmid pRG5Mc was obtained, and mobilization elements and a Gentamycin resistance cassette added, and inserted into *G. sulfurreducens,* mCherry fluorescence was observed in liquid culture. When *G. sulfurreducens* containing pRG5Mc mob-gent was grown on the electrode the growth was slower than wild type but it was faster than the *G. sulfurreducens* containing p*lac* mCherry pBBR1MCS-5 (Fig 3). Therefore, pBBR1MCS-5 was abandoned after many trials and the new plasmid, and variants, became the working plasmid.

The pRG5Mc plasmid was modified with the multiple cloning site of pBBR1MCS-5 (MCS5), the mobilization elements, and the Gentamycin resistance cassette. This plasmid was then designated pRGMCS5. This became the working plasmid for construct insertion. When the growth of *G. sulfurreducens* containing either pOmcZ mCherryLVA-pBBR1MCS-5 or pOmcZ mCherryLVA-pRGMCS5 it was clear that the *G. sulfurreducens* containing pOmcZ mCherryLVA-pRGMCS5 grew faster than the other on the electrode (Fig 4). This verified the assertion that the backbone of pRG5Mc was less detrimental for *G. sulfurreducens* growth on the electrode. The kinetics of mCherry expression in *G. sulfurreducens* was studied.

There have been no studies to date that have described the folding kinetics (total time to fluoresce) of mCherry in *G. sulfurreducens*. Most fluorescent proteins need oxygen as a cofactor, as does the mCherry that is being used, in order to oxidize the reaction center and fluoresce. Studies have shown that certain fluorescent proteins go through folding dynamics while maturing and that the presence of oxygen commits them

to fold properly and completely [42, 44, 53]. The bioreactors that *G. sulfurreducens* is grown in is anaerobic, so oxygen is not present while it is growing. This causes concern with the folding dynamics of the fluorescent proteins that require oxygen. The Lovley group has demonstrated that the expression of mCherry in anaerobic *G. sulfurreducens* biofilms leads to fluorescence when introduced to oxygen after the biofilm is established. It can be concluded that mCherry is able to fold properly in these biofilms when growing anaerobically and then fluoresce when oxygen is allowed to permeate. It important to determine how long this maturation process took before total fluorescence was reached. Liquid cultures of *G. sulfurreducens* constitutively expressing mCherry were grown anaerobically and then assayed for mCherry fluorescence. After an hour, fluorescence reached a level that was detectable over WT. However, full fluorescence occurred at approximately 4 hours (Fig 5).

It has been demonstrated that mCherry expression can occur when *G. sulfurreducens* is grown anaerobically and then allowed to oxygenate. *G. sulfurreducens* biofilms constitutively expressing mCherry on electrodes has been visualized [34]. However, it was previously unknown how long a *G. sulfurreducens* biofilm constitutively expressing mCherry needed to be in oxygen for fluorescence to be visualized via confocal microscopy [34]. The biofilms were allowed to oxidize for 1 hour in 4°C phosphate buffer without light. In liquid culture it was shown that it took mCherry approximately 4 hours to fluoresce in *G. sulfurreducens* but 1 hour oxygenation was chosen because it was assumed that biofilm integrity would be maintained and enough fluorescence to occur for visualization. The temperature was set at 4°C so that cellular

processes slowed and further degradation of mCherry would cease. When visualized, it was clear that the biofilm was expressing mCherry and red fluorescence seen throughout (Fig 6). The time allowed for oxygen was sufficient to allow the mCherry to fluoresce and became the standard time for oxygenation of the biofilms. *G. sulfurreducens* liquid cultures with both the pOmcS and pOmcZ constructs were assayed for fluorescence.

There appeared to be no notable fluorescence in any of the *G. sulfurreducens* containing the constructs when compared to the *G. sulfurreducens* constitutively expressing mCherry (Fig 7). It has been shown that the expression of certain *c*-type cytochromes increases when *G.sulfurreducens* is reducing insoluble acceptors [40]. In liquid cultures, where there is soluble acceptor, *G. sulfurreducens* expresses omcs that appear to be abundant, such as OmcZ (Rollefson, manuscript in review, 2010). It was our hypothesis that in fumarate limiting condition there would be some fluorescence of mCherryLVA when promoted by the pOmcZ and pOmcS promoters in *G. sulfurreducens*. In fumarate-limiting conditions, we believed that *G. sulfurreducens* would express more omcs in order to reduce any insoluble acceptors once the soluble acceptor is exhausted. Before being analyzed on the spectrophotometer the liquid cultures were grown to a fumarate-limiting OD (OD_{600}≈0.45-0.55). No fluorescence was detected in liquid grown cultures at late-log OD. It is unclear why no mCherryLVA fluorescence was detected but it is hypothesized that the degradation tag, LVA, is causing rapid degradation of the mCherry, so much so that fluorescence is not detected. Studies need to be done to determine the rate of degradation of mCherryLVA in *G. sulfurreducens*. Because constitutive expression of mCherry in *G. sulfurreducens* biofilms on the

electrode was demonstrated, it was assumed that any mCherryLVA expression in biofilms on the electrode would be able to be visualized. The growth of the pOmcS constructs in liquid media was explored.

The growth of constitutively expressed mCherry (pRG5Mc mob-gent) in *G. sulfurreducens* grew slower than wild type in liquid media (Fig 8). The empty plasmid, pRGMCS5, in *G. sulfurreducens* grew somewhat comparable to wild type. When the promoter region for *omcS* and variants in *G. sulfurreducens* were compared to wild type, growth was slower. Both pOmcS mCherry and pOmcS mCherryLVA in *G. sulfurreducens* were comparable with each other but showed slower growth than wild type (Fig 8). Table 3 also shows that the relative growth rates are slower with the constructs than wild type in liquid media. It is assumed that the presence of the promoter region is causing slowed growth in the liquid medium. Because the growth was slower in liquid media for the pOmcS constructs in *G. sulfurreducens* it was assumed that the same would be seen when these were grown on the electrodes.

It was assumed the promoter-reporter fusions in *G. sulfurreducens* would produce less current than wild type because of their slow growth in liquid medium. Looking at a graph of current vs. time, the *omcS* promoter-reporter constructs in *G. sulfurreducens* produced less current than wild type (data not shown). When the empty plasmid was compared to the pOmcS mCherry variants in *G.sulfurreducens* they appeared to growth similarly on the electrode (Fig 9). The addition of the degradation tag to mCherry did not appear to affect growth of *G. sulfurreducens* on the electrode. It was our belief that, with the addition of the degradation tag (AADENYLVA), the cell needs to devote energy to

degrade the tagged protein. However, because no significant difference is seen between the tagged and non-tagged mCherry in *G. sulfurreducens* it is assumed that ClpXP (protease) activity is able to manage the accumulated tagged mCherry. Therefore, it was assumed that the addition of the promoter element is the cause for the slowed growth in both liquid medium and on the electrode.

The transcriptional factors that mediate the promotion of genes may become unbalanced when a second duplicate promoter is introduced into the cell. The need for extra transcriptional factors might again divert energy production in the cell to their synthesis and to molecular control. The addition of a promoter already being regulated might also disrupt other regulatory elements that may slow the growth and metabolism of the cells. It was also hypothesized that the expression of mCherry might also be affecting the transfer of electrons to surface and electrodes. Cyclic voltammetery was done in order to determine if catalysis on the electrode was similar to wild type. The constructs in *G. sulfurreducens* showed similar characteristics on the electrode to wild type when analyzed with CV (Fig 9). Once the issues of growth were addressed, images of *G. sulfurreducens* biofilms constitutively expressing mCherry were visualized. After the growth of *G. sulfurreducens* on the electrodes and the time needed for mCherry fluorescence to occur in a biofilm were addressed a current series of *G. sulfurreducens* containing pOmcS mCherryLVA-pRGMCS5 was done.

In order to capture different developmental stages in *G. sulfurreducens* biofilm development on the electrode 4 different currents were chosen for harvesting. To represent early stage biofilm development a current of 130 μA was chosen. The biofilm

was harvested at 350 μA to represent mid-log and 630 μA to represent late-log growth. At 800 μA the biofilm reached a plateau and represented stationary phase (Fig 10). The biofilms were stained with Syto 9 and then allowed to oxygenate for 1 hour at 4°C in phosphate buffer. The biofilms were imaged and it was clear that biomass accumulated with increasing current (Fig 11). Initially, a wild type biofilm was imaged to determine the correct gain for imaging. The gain for the 561nm (red) laser was set to 6.0 in order to standardize a wild type biofilm. This remained the setting throughout imaging. The gain set at 6 allowed the image to be processed with as little background red fluorescence as possible. However, there appeared to be red fluorescence at the bottom of the biofilms (Fig 12).

When visualizing the confocal image of the wild type biofilm auto fluorescence was detected. The biofilm of *G. sulfurreducens* containing the empty vector, pRGMCS5, was imaged to check for auto fluorescence (Fig 13). A red band at the bottom of the electrode, *G. sulfurreducens* containing the empty vector also had auto fluorescence. And with each biofilm image this band occurs. Because both wild type and *G. sulfurreducens* containing the empty vector biofilm images contain autofluorescence, it is difficult to fully conclude areas of differential expression at the biofilm nearest the electrode, or whether actual mCherry fluorescence is occurring. The red auto fluorescence always occurs at the bottom of the biofilm nearest the electrode. It is hypothesized that it may be due to an artifact of the imaging process, or due to the cytochrome dynamics near the electrode.

Studies have been done to look at the fluorescence of *c*-type cytochromes. What was found was that when *c*-type cytochromes are excited with 350nm laser light they fluoresce at 402nm and 437nm [54]. This occurs when the cytochromes are reduced. When they become oxidized they lose fluorescence. Both of the emitting wavelengths correspond to the blue spectrum. However, a red band of autofluorescence is being detected. Therefore, something else must be occurring near the electrode to be causing red auto fluorescence. Another study done on *c*-type cytochrome fluorescence describes what happens when the heme group of a cytochrome begins degrading. When Fe starts to decouple from the heme group the cytochrome will emit light in the red spectrum (620-680nm) [55]. What may be occurring then near the electrode is Fe decoupling from the heme group in the cytochromes. This may due to the process of unpoising the electrode and allowing the biofilms to sit in phosphate buffer before imaging. This process may be damaging the biofilm and the areas of autofluorescence may be indicating those areas of stress. Understanding this auto fluorescence is necessary in order to distinguish mCherry expression from auto fluorescence.

G. sulfurreducens containing pOmcS mCherry-pRGMCS5 was grown on the electrode and imaged to see if mCherry expression could be observed. Figure 14 shows what looks to be mCherry expression, however, the red band is still observed at the bottom. Therefore, extreme caution needs to be employed when looking at the promoter-reporter biofilms. The current series of *G. sulfurreducens* containing pOmcS mCherryLVA-pRGMCS was visualized for mCherryLVA fluorescence. As with the

biofilms imaged before, all of the images contained the red auto fluorescence at the bottom. Studies have shown that OmcS is important in biofilms producing current.

OmcS has been shown to be important in insoluble iron reduction and in high current producing biofilms [36, 52]. Therefore, it was expected that expression mCherryLVA would be seen in the biofilms at higher currents. At 135μA, the pOmcS mCherryLVA biofilm did not appear to have any mCherryLVA fluorescence (Fig 15 A-B). Looking at the biofilm of OmcS mcLVA pRGMCS5 at 350μA reveals the same pattern as the biofilm at 135μA (Fig 15 C-D). The band is still at the bottom and no red fluorescence anywhere else in the biofilm. When the biofilm is visualized at 650μA (Fig 15 E-F) the entire biofilm appears to be red. Unlike the previous currents, it appears that there is expression of mCherryLVA occurring throughout the biofilm. At ~800μA (Fig 15 G-H) the same red fluorescence throughout is seen, even with the red band at the bottom. The higher current electrodes appear to have more mCherry expression than the lower current producing electrodes. Up until this point, the biofilms had been oxygenated for 1 hour. This time allows for mCherryLVA expression but the fluorescence cannot outcompete the auto fluorescence when the image is rendered. It was thought that the time allowed to oxygenate might need to be increased in order to allow for stronger mCherryLVA fluorescence.

The biofilms of *G. sulfurreducens* containing pOmcS mCherryLVA-pRGMCS5 were grown to a mid-log current (310 μA). Instead of a 1 hour oxygenation they were allowed to oxygenate for 3 hours under the same conditions. When the biofilm was imaged it was clear that the longer oxygenation treatment allowed for brighter

fluorescence of mCherryLVA (Fig 16 and 17). When compared to the biofilm of *G. sulfurreducens* containing pOmcS mCherryLVA-pRGMCS5 allowed to oxygenate for 1 hour it was clear that the longer oxygenation allowed the image to be rendered without the auto fluorescence.

When mCherry fluorescence is stronger than the auto fluorescence the mCherry fluorescence will be chosen as the brightest fluorescence by the imaging program and the image will be rendered so that mCherry fluorescence is the only thing is seen with the red filter. Therefore, in Figure 16, one can see that mCherryLVA expression occurs near the top of the biofilm and leads to the conclusion that expression of OmcS is occurring at the top of the biofilm at mid-log currents. Lovley et al describes OmcS transcription in biofilms on anodic surfaces. In this paper they describe the transcripts for *omcS* to be more abundant in higher current producing biofilms than in lower current producing ones. The confocal images seem to support the idea that *omcS* may be in higher transcription abundance when more current is being produced [52]. This might also reflect the importance of OmcS in developed biofilms and its function throughout.

Just recently the location and function of OmcS in has been described. Images of immunolabled OmcS show the protein festooning pili [29]. For some time it has been hypothesized that certain pili may be conductive, allowing extracellular electron transfer over distances too far for electrons to travel independently. OmcS may aid in the conductivity of these pili. It would be logical for OmcS expression to be important in late phase, or developed biofilms; aiding in extracellular conduction. The thicker a biofilm becomes the larger the distance for electrons to travel from the top of the biofilm to the

electrode. Bacteria at the top of the biofilm need to have a conductive network through the biofilm so their electrons reach the electrode. Having more OmcS produced in thick, developed biofilms would ensure that the connection to the electrode be complete. Pili may extend deep into the biofilm and it would favorable if they were lined with OmcS so those at the top may turn on expression once the biofilm reaches a certain thickness; more so than early developing biofilms. Other outer membrane cytochromes have been found to associate with the conductive extracellular matrix. One in particular, OmcZ, has been given much interest for its strong phenotype in biofilms.

Many studies have been done on the role of OmcZ in extracellular electron transfer. Gene deletions have shown how important OmcZ is in current production on electrodes. When the gene for OmcZ is knocked out current production is severely disrupted. Power output of these knockout biofilms is shown to be negligible to WT. It has also been noted that OmcZ knockouts have very thin biofilms without the pillar-like structures seen in developed WT biofilms [36]. These results demonstrate the importance of OmcZ in biofilm development and current transfer. As with *G. sulfurreducens* pOmcS mCherryLVA-pRGMCS5, the growth of *G. sulfurreducens* containing pOmcZ mCherryLVA-pRGMCS5 was determined in liquid culture.

Growth of *G. sulfurreducens* containing the pOmcZ variants was still a little slower than wild type in liquid medium (Fig 18). Looking at the relative growth rates of the constructs in *G. sulfurreducens* it is shown that their growth rates are similar amongst each other but slightly slower than wild type (Table 4). This was expected because the pOmcS variants in *G. sulfurreducens* grew slowly in liquid medium too. It was also

assumed that biofilms containing the pOmcZ constructs would grow slower on the electrode than wild type. Figure 19 demonstrates the growth of *G. sulfurreducens* containing pOmcZ mCherryLVA-pRGMCS5 on the electrode. The biofilms with the constructs grew similar to each other, much like the biofilms with pOmcS variants. It is still believed that the addition of the duplicate promoter is the cause for slowed growth. A current series was started that represented the same stages of biofilm development that were picked for the pOmcZ biofilms. The biofilms were harvested at 150 μA for early log, 325 μA for mid-log, 560 μA for late log, and 800 μA representing stationary phase (Fig 20).

The biofilm of *G. sulfurreducens* containing pOmcZ mCherryLVA-pRMGCS5 at 150 μA of current production did not appear to have any mCherry expression (Fig 21 A-B). Again, the red band near the bottom of the biofilm remained. Because of this, concluding differential expression is cautioned. When the biofilm was producing 325 μA of current a band was seen at the top of the biofilm (Fig 21 C-D). This expression was seen many times in replicates and it appears that there was expression of mCherryLVA towards the top of the biofilm at this current but the band looks similar to the auto fluorescence seen. When the biofilm reached a current production of 560 μA pockets of mCherry expression appear towards the bottom (Fig 21 E-F). These regions look like clusters of expression, not uniformly spread out like the others. The clusters correspond to high densities of cells, bright green patches, and may be areas where growth has been increased and therefore OmcZ expression higher. When the biofilm was imaged at

~800μA (Fig 21 G-H) it appears that mCherryLVA expression is occurring throughout. Again, cautionary analysis is necessary because of the auto fluorescence occurring.

A 3 hour long oxygenation seemed to be suitable for maintaining biofilm integrity and allowing for brighter fluorescence of mCherryLVA, as was the case for the biofilm of *G. sulfurreducens* containing pOmcS mCherryLVA-pRGMCS5. This was done with the biofilm of *G. sulfurreducens* containing pOmcZ mCherryLVA-pRGMCS5. When compared to the biofilm allowed to oxygenate for 1 hour it was evident that the longer oxygenation time led to more mCherryLVA fluorescence. The more brighter mCherryLVA fluorescence allowed for the auto fluorescence to be minimal, leading to the visualization of actual mCherryLVA fluorescence. The expression pattern was not uniform. Expression of mCherryLVA occurred throughout the biofilm and there were sporadic patches of expression (Fig 22 and 23). This supports that OmcZ is important throughout the biofilm during development and that OmcZ is located and distributed throughout the biofilm.

Studies done to elucidate the location of OmcZ in biofilms have been done and characterized the need for OmcZ in biofilms. Microtoming done on an electrode that was approximately 60μm thick revealed that there was no differential expression in the biofilm. However, the microtoming allowed for transcriptional data to be collected from the inner biofilm (0-20μm) and the outer biofilm (30-60μm) [37]. What was noticed in an earlier study was that OmcZ was in higher transcriptional abundance in high current producing biofilms [7, 56]. This may be reflected in the images for OmcZ. There was not an extremely noticeable difference in mCherry expression in early to late biofilms.

Expression of mCherry was unpredictable. If this is the case one can conclude that OmcZ may be important throughout the biofilm and is not differentially expressed but always highly expressed. Immunolabeling OmcZ has also shown that it is a part of the extracellular matrix, much like OmcS, and that it is a major contributor to current production in biofilms [56]. This further supports the idea that OmcZ may be highly expressed throughout biofilm development and more highly expressed when regions of the biofilm are growing rapidly, which is seen in the confocal images.

The confocal images gathered have shown that through the use of promoter-reporter fusions gene expression may be visualized in a developing *G. sulfurreducens* biofilm. The promoter-reporter data has begun to support the importance of OmcS and OmcZ in developing biofilms and their roles in current production. This system has shown promise in elucidating differential expression, however, it needs refinement and special attention taken to auto fluorescence.

Chapter 3

Conclusions and Future Directions

The aim of this project was to discover a new method for determining gene expression in *G. sulfurreducens* biofilms when grown on graphite electrodes. As it has been stated throughout, there have been many methods employed to determine and visualize gene expression in these biofilms. However, most of these are global methods. None give the resolution that can be obtained through visualizing reporters via microscopy. Utilizing promoter-reporters one can visualize gene expression on a micron scale. With the addition of a degradation tag to the end of a reporter the expression can be visualized over time, not only spatially. This system appeared to work in *G. sulfurreducens* biofilms on electrodes. There were and still are problems with the system in *Geobacter*. The fluorophore used in these promoter-reporter fusions requires oxygen and *G. sulfurreducens* biofilms are anaerobic. This may lead to a misfolding of the majority of mCherry being translated. Oxygen is purposefully excluded from the bioreactors so high currents can be reached and therefore total mCherry fluorescence mostly likely does not occur. Not only is mCherry visualization hindered by the lack of oxygen but it also appears that the cytochromes in the biofilm auto fluoresce when using the 561nm (red) laser.

Most of the images gathered throughout the project have a red band of false mCherry fluorescence at the electrode surface. When compared to EGFP, mCherry only has 41% the relative brightness. That, along with the lack of oxygen, leads to a dim fluorescence of mCherry. When visualized with confocal auto correction is used to

brighten the image. The program picks the brightest "red" and intensifies the remaining "red" with regards to that level. Therefore, the auto fluorescence of the biofilm causes the program to intensify them. It is hard to then determine if there is expression occurring at the electrode level of the biofilm or if it is an artifact of auto fluorescence. To get past these issues different modifications are being looked at.

One thing that is being investigated is the use of a tagged EGFP (EGFP-LVA) fused to the promoters of interest. This, along with a red nucleic acid stain (Syto62), would give the same spectral difference when viewing but eliminate the red auto fluorescence of the biofilm. To circumvent the oxygen requirement of the fluorophore, a new system in which the reaction center of the fluorphore is oxidized by FMN rather than oxygen is being investigated [57]. This would allow the biofilms to remain anaerobic and unmanipulated until imaging; possibly maintaining more of the biofilm integrity as well. These modifications to the promoter-reporter system used in these studies may give more insight into the expression of outer membrane cytochromes in *G. sulfurreducens* biofilms on graphite electrodes.

References

1. Parsek, M.R. and P.K. Singh, *Bacterial biofilms: an emerging link to disease pathogenesis.* Annu Rev Microbiol, 2003. **57**: p. 677-701.
2. Lovley, D.R., *Dissimilatory metal reduction.* Annu Rev Microbiol, 1993. **47**: p. 263-90.
3. Bond, D.R. and D.R. Lovley, *Electricity production by Geobacter sulfurreducens attached to electrodes.* Appl Environ Microbiol, 2003. **69**(3): p. 1548-55.
4. Caccavo, F., et al., *Geobacter Sulfurreducens Sp-Nov, a Hydrogen-Oxidizing and Acetate-Oxidizing Dissimilatory Metal-Reducing Microorganism.* Applied and Environmental Microbiology, 1994. **60**(10): p. 3752-3759.
5. Methe, B.A., et al., *Genome of Geobacter sulfurreducens: metal reduction in subsurface environments.* Science, 2003. **302**(5652): p. 1967-9.
6. Izallalen, M., et al., *Geobacter sulfurreducens strain engineered for increased rates of respiration.* Metab Eng, 2008. **10**(5): p. 267-75.
7. Nevin, K.P., et al., *Anode biofilm transcriptomics reveals outer surface components essential for high density current production in Geobacter sulfurreducens fuel cells.* Plos One, 2009. **4**(5): p. e5628.
8. Inoue, K., et al., *Purification and characterization of OmcZ, an outer-surface, octaheme c-type cytochrome essential for optimal current production by Geobacter sulfurreducens.* Appl Environ Microbiol. **76**(12): p. 3999-4007.
9. Leang, C., et al., *Alignment of the c-type cytochrome OmcS along pili of Geobacter sulfurreducens.* Appl Environ Microbiol. **76**(12): p. 4080-4.
10. Franks, A.E., et al., *Microtoming coupled to microarray analysis to evaluate the spatial metabolic status of Geobacter sulfurreducens biofilms.* ISME J. **4**(4): p. 509-19.
11. Inoue, K., et al., *Specific localization of the c-type cytochrome OmcZ at the anode surface in current-producing biofilms of Geobacter sulfurreducens.* Environmental Microbiology Reports: p. no-no.
12. Monds, R.D. and G.A. O'Toole, *The developmental model of microbial biofilms: ten years of a paradigm up for review.* Trends Microbiol, 2009. **17**(2): p. 73-87.
13. Teal, T.K., et al., *Spatiometabolic stratification of Shewanella oneidensis biofilms.* Appl Environ Microbiol, 2006. **72**(11): p. 7324-30.
14. Zaslaver, A., et al., *A comprehensive library of fluorescent transcriptional reporters for Escherichia coli.* Nat Methods, 2006. **3**(8): p. 623-8.
15. Logan, B.E. and J.M. Regan, *Microbial fuel cells--challenges and applications.* Environ Sci Technol, 2006. **40**(17): p. 5172-80.
16. Logan, B.E., *Exoelectrogenic bacteria that power microbial fuel cells.* Nat Rev Microbiol, 2009. **7**(5): p. 375-81.
17. Logan, B.E., et al., *Microbial fuel cells: methodology and technology.* Environ Sci Technol, 2006. **40**(17): p. 5181-92.
18. Lovley, D.R., *Dissimilatory Fe(III) and Mn(IV) reduction.* Microbiol Rev, 1991. **55**(2): p. 259-87.

19. Lovley, D.R., D.E. Holmes, and K.P. Nevin, *Dissimilatory Fe(III) and Mn(IV) reduction.* Advances in Microbial Physiology, Vol. 49, 2004. **49**: p. 219-286.
20. Lovley, D.R., *Bioremediation of organic and metal contaminants with dissimilatory metal reduction.* J Ind Microbiol, 1995. **14**(2): p. 85-93.
21. Lloyd, J.R. and D.R. Lovley, *Microbial detoxification of metals and radionuclides.* Current Opinion in Biotechnology, 2001. **12**(3): p. 248-253.
22. Moser, C.C., et al., *Distance metrics for heme protein electron tunneling.* Biochim Biophys Acta, 2008. **1777**(7-8): p. 1032-7.
23. Weber, K.A., L.A. Achenbach, and J.D. Coates, *Microorganisms pumping iron: anaerobic microbial iron oxidation and reduction.* Nature Reviews Microbiology, 2006. **4**(10): p. 752-764.
24. Du, Z., H. Li, and T. Gu, *A state of the art review on microbial fuel cells: A promising technology for wastewater treatment and bioenergy.* Biotechnol Adv, 2007. **25**(5): p. 464-82.
25. Reguera, G., et al., *Extracellular electron transfer via microbial nanowires.* Nature, 2005. **435**(7045): p. 1098-1101.
26. Reguera, G., et al., *Biofilm and nanowire production leads to increased current in Geobacter sulfurreducens fuel cells.* Appl Environ Microbiol, 2006. **72**(11): p. 7345-8.
27. Reguera, G., et al., *Possible nonconductive role of Geobacter sulfurreducens pilus nanowires in biofilm formation.* J Bacteriol, 2007. **189**(5): p. 2125-7.
28. Lovley, D.R., *Extracellular electron transfer: wires, capacitors, iron lungs, and more.* Geobiology, 2008. **6**(3): p. 225-231.
29. Leang, C., et al., *Alignment of the c-Type Cytochrome OmcS along Pili of Geobacter sulfurreducens.* Applied and Environmental Microbiology, 2010. **76**(12): p. 4080-4084.
30. Bond, D.R. and D.R. Lovley, *Electricity production by Geobacter sulfurreducens attached to electrodes.* Applied and Environmental Microbiology, 2003. **69**(3): p. 1548-1555.
31. Marsili, E., et al., *Microbial Biofilm Voltammetry: Direct Electrochemical Characterization of Catalytic Electrode-Attached Biofilms.* Applied and Environmental Microbiology, 2008. **74**(23): p. 7329-7337.
32. Lovley, D.R., et al., *Geobacter-Metallireducens Gen-Nov Sp-Nov, a Microorganism Capable of Coupling the Complete Oxidation of Organic-Compounds to the Reduction of Iron and Other Metals.* Archives of Microbiology, 1993. **159**(4): p. 336-344.
33. Caccavo, F., Jr., et al., *Geobacter sulfurreducens sp. nov., a hydrogen- and acetate-oxidizing dissimilatory metal-reducing microorganism.* Appl Environ Microbiol, 1994. **60**(10): p. 3752-9.
34. Franks, A.E., et al., *Novel strategy for three-dimensional real-time imaging of microbial fuel cell communities: monitoring the inhibitory effects of proton accumulation within the anode biofilm.* Energy & Environmental Science, 2009. **2**(1): p. 113-119.

35. Ding, Y.H., et al., *Proteome of Geobacter sulfurreducens grown with Fe(III) oxide or Fe(III) citrate as the electron acceptor.* Biochim Biophys Acta, 2008. **1784**(12): p. 1935-41.
36. Nevin, K.P., et al., *Anode Biofilm Transcriptomics Reveals Outer Surface Components Essential for High Density Current Production in Geobacter sulfurreducens Fuel Cells.* Plos One, 2009. **4**(5): p. -.
37. Franks, A.E., et al., *Microtoming coupled to microarray analysis to evaluate the spatial metabolic status of Geobacter sulfurreducens biofilms.* Isme Journal, 2010. **4**(4): p. 509-519.
38. Juarez, K., et al., *PilR, a Transcriptional Regulator for Pilin and Other Genes Required for Fe(III) Reduction in Geobacter sulfurreducens.* Journal of Molecular Microbiology and Biotechnology, 2009. **16**(3-4): p. 146-158.
39. Methe, B.A., et al., *Genome of Geobacter sulfurreducens: Metal reduction in subsurface environments.* Science, 2003. **302**(5652): p. 1967-1969.
40. Mehta, T., et al., *Outer membrane c-type cytochromes required for Fe(III) and Mn(IV) oxide reduction in Geobacter sulfurreducens.* Applied and Environmental Microbiology, 2005. **71**(12): p. 8634-8641.
41. Holmes, D.E., et al., *Microarray and genetic analysis of electron transfer to electrodes in Geobacter sulfurreducens.* Environ Microbiol, 2006. **8**(10): p. 1805-15.
42. Southward, C.M. and M.G. Surette, *The dynamic microbe: green fluorescent protein brings bacteria to light.* Mol Microbiol, 2002. **45**(5): p. 1191-6.
43. Sternberg, C., et al., *Distribution of bacterial growth activity in flow-chamber biofilms.* Appl Environ Microbiol, 1999. **65**(9): p. 4108-17.
44. Andersen, J.B., et al., *New unstable variants of green fluorescent protein for studies of transient gene expression in bacteria.* Appl Environ Microbiol, 1998. **64**(6): p. 2240-6.
45. Qu, Y., et al., *GSEL version 2, an online genome-wide query system of operon organization and regulatory sequence elements of Geobacter sulfurreducens.* OMICS, 2009. **13**(5): p. 439-49.
46. Kovach, M.E., et al., *Four new derivatives of the broad-host-range cloning vector pBBR1MCS, carrying different antibiotic-resistance cassettes.* Gene, 1995. **166**(1): p. 175-6.
47. Rollefson, J.B., C.E. Levar, and D.R. Bond, *Identification of Genes Involved in Biofilm Formation and Respiration via Mini-Himar Transposon Mutagenesis of Geobacter sulfurreducens.* Journal of Bacteriology, 2009. **191**(13): p. 4207-4217.
48. Saltikov, C.W. and D.K. Newman, *Genetic identification of a respiratory arsenate reductase.* Proc Natl Acad Sci U S A, 2003. **100**(19): p. 10983-8.
49. Shaner, N.C., et al., *Improved monomeric red, orange and yellow fluorescent proteins derived from Discosoma sp. red fluorescent protein.* Nat Biotechnol, 2004. **22**(12): p. 1567-72.
50. Coppi, M.V., et al., *Development of a genetic system for Geobacter sulfurreducens.* Applied and Environmental Microbiology, 2001. **67**(7): p. 3180-3187.

51. Qiu, Y., et al., *Structural and operational complexity of the Geobacter sulfurreducens genome.* Genome Res. **20**(9): p. 1304-11.
52. Holmes, D.E., et al., *Microarray and genetic analysis of electron transfer to electrodes in Geobacter sulfurreducens.* Environmental Microbiology, 2006. **8**(10): p. 1805-1815.
53. Andrews, B.T., et al., *The dual-basin landscape in GFP folding.* Proc Natl Acad Sci U S A, 2008. **105**(34): p. 12283-8.
54. Esteve-Nunez, A., et al., *Fluorescent properties of c-type cytochromes reveal their potential role as an extracytoplasmic electron sink in Geobacter sulfurreducens.* Environmental Microbiology, 2008. **10**(2): p. 497-505.
55. Fraaije, J.G., et al., *Orientation of adsorbed cytochrome c as a function of the electrical potential of the interface studied by total internal reflection fluorescence.* Biophys J, 1990. **57**(5): p. 965-75.
56. Inoue, K., et al., *Purification and Characterization of OmcZ, an Outer-Surface, Octaheme c-Type Cytochrome Essential for Optimal Current Production by Geobacter sulfurreducens.* Applied and Environmental Microbiology, 2010. **76**(12): p. 3999-4007.
57. Drepper, T., et al., *Flavin mononucleotide-based fluorescent reporter proteins outperform green fluorescent protein-like proteins as quantitative in vivo real-time reporters.* Appl Environ Microbiol. **76**(17): p. 5990-4.